LOS ALAMOS NATIONAL LABORATORY

ACTINIDE RESEARCH QUARTERLY

4th Quarter 2008/1st Quarter 2009

Plutonium Futures

The Science 2008

DIJON, FRANCE

Los Alamos NATIONAL LABORATORY EST.1943

Contents

Plutonium Futures—The Science 2008

About the cover

Dijon and the region of Burgundy are famous not only for mustard and wine but for the beautiful "toits bourguignons" (Burgundian roofs) of colorful glazed tiles arranged in geometric patterns.

SUPPORTING SAFE AND SECURE NUCLEAR RESEARCH AS PART OF THE WORLD ENERGY MIX

Plutonium Futures—The Science has become an important international forum in which scientists, engineers, and students from universities, national laboratories, and nuclear complexes may openly discuss current and emerging topics in plutonium and associated actinide science. The conference, initiated by Los Alamos and Lawrence Livermore National Laboratories, had previously been held in Santa Fe, New Mexico, in 1997 and 2000; Albuquerque, New Mexico, in 2003; and Asilomar, California, in 2006.

The international scope of the conference was recognized by the Organizing Committee in its support of a proposal by a European consortium to bring the conference to Europe in July 2008. Dijon, the capital of Burgundy in France, was chosen as the host city for the fifth Plutonium Futures conference.

The conference, which was held July 7-11 at the Dijon Convention Centre, was organized by the European consortium—the French Atomic Energy Commission (CEA), the Institute for Transuranium Elements of the European Commission (ITU), and the Atomic Weapon Establishment of the United Kingdom (AWE)—and sponsored by the European Commission, AREVA, the Côte d'Or Region, and the Pole Nucléaire de Bourgogne. This year's conference

The château (above) at the Clos de Vougeot vineyards in Burgundy was the site of the official banquet. Right, from top to bottom: conference chairman Claude Guet (left) and honorary chairman Gerry Lander, conference chairmen David Geeson (standing at left) and Thomas Fanghänel (standing at right), and honorary chairman Sig Hecker.

Clockwise from top: Dijon at night; conference attendees gather in the château courtyard for an official photo; Jean Fuger, professor emeritus, University of Liège, Belgium, and his dog, Cookie, arrive at the château.

attracted 330 attendees from 19 countries; the United States had the largest delegation from outside Europe.

Plenary lectures were delivered at the beginning of each session. Oral contributions were presented in two parallel sessions, and ample space was given to daily poster sessions. The scientific program encompassed a broad range of issues relating to condensed-matter physics, chemistry, safety, nuclear waste management, nuclear fuel cycles, surface and corrosion phenomena, speciation, and analytical methods.

Among the highlights of the week were discussions of Dynamical Mean Field Theory calculations, which have reached a level of sophistication that allows for detailed understanding of the electronic structure of plutonium. Debated topics included competition between spin-orbit and exchange interactions, electronic coherence effects, spin fluctuations, and quantum criticality in delta (δ)-plutonium. Interesting new experimental results on elemental plutonium were presented based on inelastic neutron scattering, photoemission spectroscopy, and electron energy-loss spectroscopy. The long-standing problem of the transition from localized to delocalized 5f-electrons was addressed in several talks.

Another topic that attracted interest during the conference was that of exotic magnetism and superconductivity in strongly correlated 5f electron systems. Several talks were dedicated to unconventional uranium-, plutonium-, and neptunium-based superconductors. The nature of the pairing bosons in these materials remains to be determined and is a central issue in current condensed-matter physics.

The materials science and fuel-cycle sessions were particularly informative. The stabilization of the face-centered cubic plutonium δ-phase remains of considerable interest, and the role of lattice defects accumulated over many years of self-irradiation has been thoroughly investigated. Advanced numerical

simulations have opened the way to a predictive understanding of atomic-scale processes and helium-vacancy interactions in nuclear fuel materials. A comprehensive review of plutonium-containing fuel for sodium-cooled fast breeders and burners was presented in a plenary talk. Other discussions included new methods of preparing fuels containing minor actinides, their thermochemical and thermophysical properties, and the proliferation-resistant characteristics of nuclear fuels.

Advances in understanding the extremely complex chemical behavior of plutonium and other actinides were described in many submissions, including experimental and theoretical approaches. The discussions ranged from actinide hydration, hydrolysis, and aggregation to the redox chemistry of uranium, neptunium, and plutonium compounds in controlled conditions. Thermodynamic studies of the complexation of plutonium by different ligands were presented, as well as studies concerning the interaction of actinides with peptides and proteins.

Other topics were related to the solubility of plutonium in molten salts, the formation and stability of actinide oxides, the formation of Pu(IV) colloids, and the formation and hydrolysis of An(IV) polynuclear complexes. Case histories of nuclear materials confiscations and the successful application of nuclear forensic investigation methods to the identification of their origin were presented in the speciation, analysis and detection session, together with analysis methods based on laser-induced spectroscopy. Environmental issues included the measurements of plutonium traces in atmospheric precipitations and the study of the impact assessment in the case of an accidental atmospheric release.

Societal aspects and public perceptions of plutonium were at the heart of round table discussions, one on global security and the other on environmental concerns. The lively debate between scientists and policy makers highlighted clearly how science and society are strongly coupled.

The conference participants were given the opportunity to visit one of the temples of the French gastronomy, Clos de Vougeot, where a memorable banquet took place in the Renaissance atmosphere of a beautiful château surrounded by one of the most famous vineyards of Burgundy. The banquet was introduced by welcome addresses from Jacques Bouchard, chairman of the Generation IV Forum, and Philippe Garderet, scientific director of AREVA. Sig Hecker and Gerry Lander, the honorary chairmen of the conference, had the honor of delivering after-dinner speeches; as always, they were brilliant and illuminating.

—Claude Guet (CEA), Thomas Fanghänel (ITU), and David Geeson (AWE)
Plutonium Futures 2008 conference chairmen

From top to bottom: Another view of Dijon at night; Jacques Bouchard, chairman of the Generation IV Forum; Philippe Garderet, scientific director of AREVA.

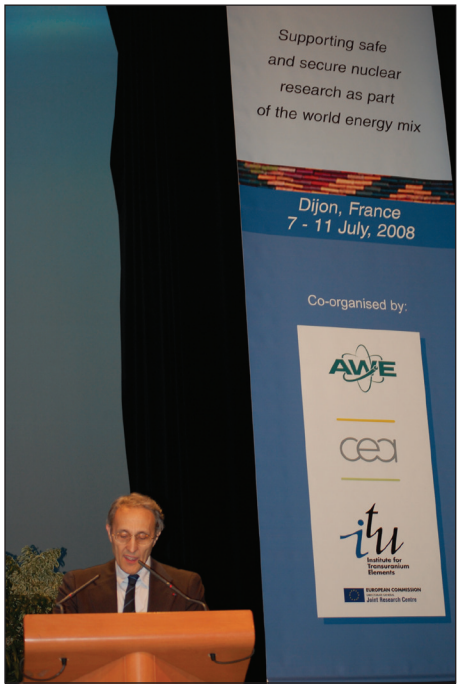

Bernard Bigot, French High Commissioner for Atomic Energy.

Opening Remarks

It is an honor and my pleasure as the French High Commissioner for Atomic Energy to open the fifth Plutonium Futures—The Science Conference and to welcome all of you—with a special acknowledgment of our foreign visitors—to Dijon in the heart of Burgundy, a region famous for its hospitality and the quality of its architecture, food, and wine.

This is the first time this conference series has come to Europe. The series started in 1997 in Santa Fe, New Mexico, in the United States. Dr. Hecker, at that time director of Los Alamos National Laboratory, wished to gather scientists from different backgrounds and experience but with one thing in common—the study of plutonium science. The objectives were clear: to promote research in the field, to attract bright young scientists, to develop international exchanges, and to further the knowledge of plutonium properties in an open manner while precluding the spread of sensitive information.

I personally see three major reasons for the success of the previous conferences and the expected success of this one: the challenges we face with the growing demand for energy, the concern about nuclear security and proliferation, and the uniqueness of plutonium itself.

The first major expectation for this year's conference is associated with the progress that could be made—and the immense challenges we face—on energy issues. What is at stake is the need to satisfy the increased energy needs of the world due to the growing population and the improvement in the conditions of life for many people while drastically reducing the impact on the climate of primary energy consumption.

The overwhelming evidence for the rapid warming of the climate caused by increased greenhouse gas emissions is alarming and calls for major international changes in the world's energy policies. Efforts to save energy are the priority, but they will not be sufficient. A drastic reduction of the use of fossil resources is mandatory, even without considering the fact that these fossil resources are expected to be largely exhausted before the end of this century and will become more and more expensive to extract.

Major efforts in research and development ought to be devoted to the worldwide growth of clean energies such as solar for heat and electricity, wind, hydrogen-based technologies, third-generation biomass transformation to biofuels, and others. In spite of these imperative efforts, alternative energies cannot by any means comply with the world's needs in the near future because they suffer from intermittency and diffuse features, as well as from technological limitations on efficient energy storage. The deployment of alternative energies will be efficient only if there is a steady energy supply that not only is free of greenhouse gas emission but also is benign to the environment.

Today, from the viewpoint of more and more people, there is only one way to ensure a steady energy supply in the coming decades: nuclear fission and the

deployment of nuclear power plants on a larger scale. Even at a steady rate of expansion of about 20 new reactors per year, it will take many years to really impact climate change. However, uranium resources are also limited, and current thermal neutron reactors are ashamedly inefficient at burning uranium; they take advantage of less than 0.6% of the energy content of the natural ore.

There are clearly identified ways for a much more efficient use of fissile and fertile materials. The route is by combining fast-neutron reactors with a closed fuel cycle. France and partners from the Generation IV forum are actively working on these technologies. In addition to optimizing nuclear fuel combustion, these technologies will favor the reduction of nuclear waste.

The nuclear element that is at the heart of these new technologies is plutonium. Plutonium does not exist in nature, or only at an extremely low level, but is produced in uranium nuclear reactors after neutron capture by uranium-238. Plutonium-239 is a very energetic fissile material that in turn can be used as fresh fuel, after reprocessing the spent uranium fuel.

There is much work to do on the behavior of various fuels in fast reactors depending upon their chemical features (oxide, carbide, nitride, or metal), transient processes, burn-up rate, confinement, and interaction with cladding. Chemists are developing methods to improve the separation processes. I know that some of you here this week will present recent advances in this research.

I mentioned the waste issue. It is a major issue for assessing the public's acceptance of the development of nuclear energy in all countries. We scientists have an essential role to play by assessing the safety of various storage methods inside various geological media over long periods of time. I appreciate the scientific hurdles, as we are talking of the evolution of complex systems over hundreds of thousands of years, thus requiring a strong and guaranteed predicting power.

The second major expectation from this conference has to do with the serious worldwide issues of security and proliferation. How shall we make sure that an extensive deployment of civil peaceful nuclear energy will be conducted over all five continents without any risk of diversion by a state for a covert nuclear weapons program or by a terrorist organization?

As to plutonium itself, the highest attention ought to be paid to identify it: where it came from and who made it. In addition to political and institutional agreements between fuel suppliers and fuel users, new standards of safety need to be implemented as well as efficient remote monitoring of fuel facilities and reactors. These technologies are science-based and the research that some of you here are carrying out is of paramount importance.

The third major reason for you to meet here is to share your excitement about the subtleties of plutonium and plutonium compounds, the extraordinary richness of physics that they exhibit, and their unconventional chemical and metallurgical behavior. Indeed, plutonium is quite unique. Sig Hecker once defined plutonium as "the dream of physicists and the nightmare of metallurgists."

The reactors of the Tricastin EDF nuclear site near Bolène as seen from a car window on a motor trip from Dijon to Aix-en-Provence.

This conference is also unique in that physicists, chemists, metallurgists, and environmental scientists may tell each other their dreams and nightmares about plutonium's properties and not get scared by them but instead are encouraged to cooperate to solve these intellectually challenging questions. I expect some significant progress in the role of the correlated electron dynamics in the anomalous properties of the alpha (α) and delta (δ) phases. I also expect significant advances on the chemistry of plutonium compounds in various media, on the physicochemistry at interfaces, on the corrosion processes, and on the thermodynamic properties—without excluding some surprises.

My last words will be to wish you an exciting meeting, fruitful scientific exchanges, and new friendships.

—Bernard Bigot, French High Commissioner for Atomic Energy

Inside the Dijon Convention Center (top), Catherine Treimany of CEA/Valduc introduces the opening session speakers (bottom).

HIGH-PLUTONIUM-CONTENT FUELS: CHALLENGES IN SCIENCE AND TECHNOLOGY

This article was contributed by Baldev Raj, director, Indira Gandhi Center for Atomic Research (IGCAR).

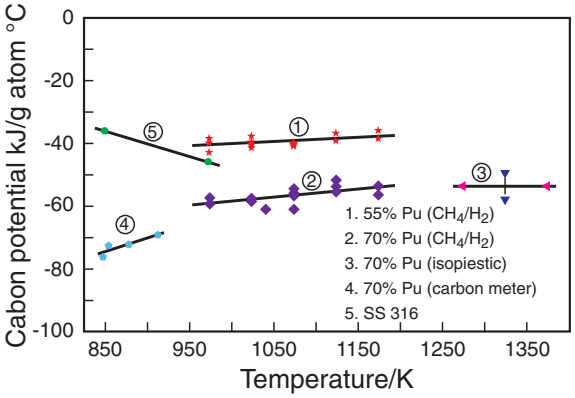

At left: Carbon potentials of Mark I and Mark II (uranium, plutonium) mixed carbide fuel.

In the early 1980s, India made the choice to use a uranium–plutonium (U–Pu) mixed-carbide fuel with a high plutonium content as the driver fuel for the Fast Breeder Test Reactor at Kalpakkam, which is a 40-megawatt loop-type, sodium-cooled fast reactor. It was obvious that many challenges would be faced in the manufacturing, performance, and reprocessing of the fuel. Reactor physics considerations indicated that the fuel would have a Pu/U + Pu ratio of 0.55 to 0.7, depending on the core size (higher plutonium content of 0.7 for small core configuration).

There was no experience with this fuel anywhere in the world, and little data on thermophysical and thermochemical properties were available in the literature. A bold—but considered safe—decision was made to proceed with design of the fuel by a combination of experimentation and modeling. The pyrophoricity of the fuel required a high-purity inert gas environment for characterization and manufacturing. The melting point of the fuel could be measured by incipient melting technique, and thermal conductivity could be measured by laser flash technique.

The composition of the fuel in terms of its oxygen and nitrogen content and the carbon-to-metal ratio would be vital parameters that would influence the performance. The carbon potential of the fuel had to be understood for the compositions of the fuel and also in terms of the concentration of oxygen and nitrogen as a function of temperature. The carbon potential of the fuel was measured for specific compositions by methane–hydrogen gas equilibration technique, isopiestic method, and molten salt electromotive force measurement.

The carbon potential of the mixed-carbide fuel with Pu/(U + Pu) = 0.70 was found to be lower than that of stainless steel and thus, no carburization of the cladding was expected. The carbon potential of fuel with Pu/(U + Pu) = 0.55 was comparable with that of stainless steel, but once again, because the carbon monoxide pressures measured over the fuel were only around 10^{-2} pascal at the operating temperatures (900–1300 K) of the fuel, carbon transport to the cladding from the fuel would be insignificant.

The inert atmosphere hot cell facility in the Radiometallurgy Laboratory at IGCAR.

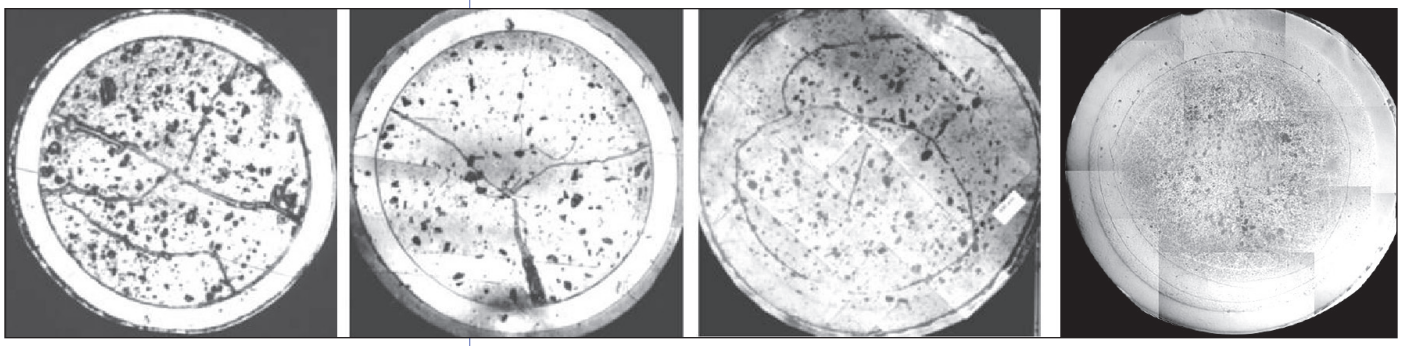

Ceramographs of fuel-clad cross sections at various burnups at (from left to right) 25 GWd/tHM, 50 GWd/tHM, 100 GWd/tHM, and 154 GWd/tHM.

The exchange reaction between the sesquicarbide, $(Pu,U)_2C_3$, and monocarbide, (Pu,U)C, phases involves a more-negative free-energy change with increasing plutonium content. Thus, the carbide fuel with higher plutonium content would have a lower carbon potential. These data, along with the modeling of the carbon potential of the fuel using the free-energy minimization approach, provided the scientific basis that the carbide fuel would be compatible with cladding.

The choice of fuel specifications (5%–15% sesquicarbide content, <5000 parts per million of oxygen) has been vindicated by excellent performance of the fuel. The irradiation performance of the carbide fuel has been assessed using a host of destructive and nondestructive techniques specially established in inert atmosphere hot cells at various stages of burnups of 25, 50, 100, and 154 gigawatt-days per metric ton of heavy metal (GWd/tHM).

Axial and radial fuel swelling was measured after different burnups using nondestructive and destructive techniques. Percentage increase in fuel stack length, pellet-to-pellet gap, and pellet-to-clad gap were estimated using X-ray and neutron radiography. Even though the melting temperature of mixed carbide with 70% PuC is much lower (2100 K) than that of the fuel with 20% PuC (2750 K), the choice of lower operating temperature and appropriate linear heat rating resulted in lower swelling rates even at high burnup.

Ceramography of fuel cross sections at lower burnups indicated a free swelling regime as evident from the radial cracking patterns and observed post-irradiation fuel-cladding gap. With increasing burnup beyond 50 GWd/tHM, the cracking pattern changed to circumferential with the closure of the fuel-cladding gap, indicating a restrained swelling phase. A progressive reduction in the porosities was observed on the fuel microstructure with increasing burnups.

At the burnup of 154 GWd/tHM, distinct porosity-free peripheral zones were observed in the fuel. This indicated that the creep behavior of the plutonium-rich carbide fuel resulted in accommodation of the swelling in the fuel-clad mechanical interaction regime.

The measured cladding strains were also found to be predominantly from the void swelling of the stainless steel cladding material (CW ASS316), which was also substantiated by modeling of the creep and swelling behavior of the fuel and the cladding material.

The challenge of the high-plutonium-content carbide fuel was even more accentuated in reprocessing of the fuel. The carbide fuel was reprocessed by the PUREX process, involving dissolution of the fuel in nitric acid followed by a solvent extraction process employing tri-n-butyl phosphate (TBP) dissolved in n-dodecane diluent. It is well known that the extraction of high concentrations of tetravalent actinides, including Pu(IV), by TBP in hydrocarbon diluents leads to the splitting of the organic phase into two organic phases (a phenomenon called "third-phase formation").

The third phase—the heavier organic phase—is rich in the extractant and the metal/acid-solvate, while the lighter organic phase essentially comprises the diluent and traces of extractant and metal/acid-solvate. Third-phase formation in the solvent extraction process can cause hydrodynamic disturbances in the contactors leading to flooding as well as criticality problems, because the concentration of plutonium in the third phase can be as high as 1.5 molar. Therefore, it is important to obtain a comprehensive understanding of the phenomenon by measuring the limiting organic concentration (LOC) for avoiding third-phase formation, as a function of various parameters such as aqueous acidity, TBP concentration, and presence of uranium.

Modeling of the effect of the variation in operating conditions on plutonium concentration in the organic phase, combined with the data on LOC, provided critical inputs that enabled the delineation of adequate and safe operating conditions for reprocessing. For example, it could be demonstrated that by using two strip solutions with optimized flow rates, it is possible to ensure that the maximum plutonium concentration in the organic phase will remain within the LOC.

Studies on thorium (Th) extraction by a variety of trialkyl phosphates gave a clear indication that trialkyl phosphates with longer carbon chains have higher LOC for third-phase formation for thorium. A similar behavior was expected for plutonium. In fact, initial experiments indicated that it is very difficult to induce third-phase formation in plutonium extraction by the triamyl phosphate system. These implied that trialkyl phosphates with carbon chains longer than four carbon units would be more suitable for reprocessing fast-reactor fuels with high plutonium content.

Interestingly, measurements on tracer-level plutonium extraction by trialkyl phosphates showed that the distribution coefficient for extraction of Pu(IV) or U(VI) does not vary significantly with increase in alkyl chain length. The presence of uranium in the organic phase reduces the limit of tolerable plutonium concentration. An increase in the TBP concentration, use of a hydrocarbon diluent with shorter carbon chains, and higher temperature all lead to a higher LOC. An increase in the LOC implies that a higher plutonium loading in the organic phase can be tolerated, which means higher plant throughputs and also less extraction of fission products because the free-extractant concentration would be reduced.

Variation of maximum organic phase concentration of plutonium with nitric-acid concentration in strip solutions.

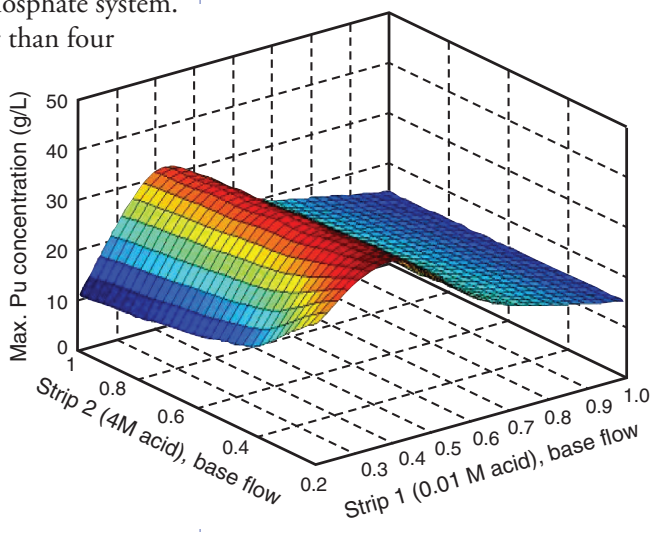

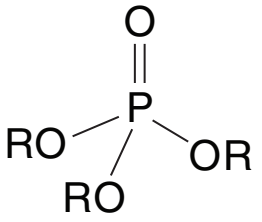

R = n-butyl or cyclyhexyl
When R = butyl, this is
the TPB ligand

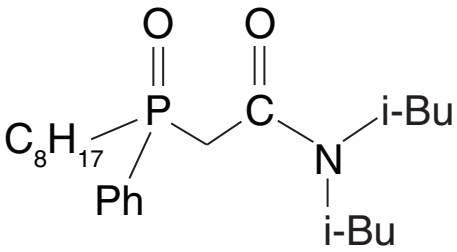

CMPO

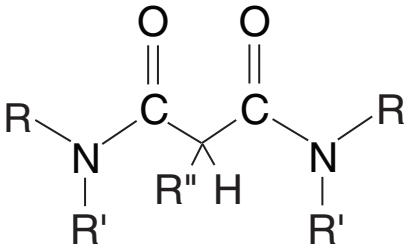

Malonamide

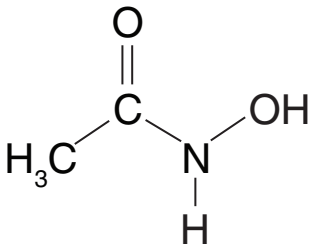

AHA

With the knowledge that third-phase formation is not limited to trialkyl phosphates, but also exists with a host of other extractants—octyl(phenyl)-N,N-diisobutylcarbamylmethylphosphinoxide (CMPO), used for minor actinide extraction from nitric acid media, and dialkyl monamides as well as malonamides—the importance of this phenomenon is generic. The fact that the LOC for Th(IV) for extraction by TBP decreases with increase in nitric-acid concentration while that for extraction of Pu(IV) by TBP increases with nitric-acid concentration after an initial decrease highlights the difference between plutonium and thorium in terms of formation of multiple species in organic phase.

While third-phase formation is now understood in terms of reverse micelle formation in the extractant phase, much more experimentation is needed before a comprehensive understanding is reached on this subject. The behavior of tricyclohexyl phosphate, which forms third phase even with uranium, for example, needs to be studied in more detail.

The extensive modeling of the extraction processes has provided crucial inputs to the development of the solvent extraction flow sheet for fast breeder test reactor fuel reprocessing. The SIMPSEX computer code, developed in house and benchmarked extensively using published flow sheets, was used for modeling the solvent extraction of uranium, plutonium, nitric acid, and others, as well as to predict third-phase formation during extraction. The SIMPSEX code has also been used for studying coprocessing options for uranium and plutonium for commercial-scale reprocessing plants.

Models for accurately predicting densities of plutonium-containing solutions and extraction behavior with the use of an acetohydroxamic acid (AHA) complexing agent have also been developed. It can now be said that flow sheets for reprocessing plutonium-rich fuels can be developed with only essential experimentation.

The choice of high-plutonium-content carbide fuel has provided many challenges and opportunities for research and development in plutonium science and technology and enabled appreciation of the influence of plutonium content on the properties, performance, and fuel cycle of carbide fuels. The investigations have also formed a strong base for establishing inert atmosphere facilities for research and development on all advanced fuels, including metallic fuels and fuels incorporating minor actinides for burning in fast reactors.

PLUTONIUM ALLOYS UNDER PRESSURE

This article was contributed by Philippe Faure, Claudine Genestier, and François Delaunay, Atomic Energy Commission (CEA), Valduc.

Plutonium is well known for exhibiting physical properties that challenge—even 60 years after its discovery, and despite intensive investigation by theorists and metallurgists. As new techniques are developed to understand the mystery of plutonium, new subtleties or details are being revealed. We report here on new insights regarding the behavior of plutonium alloys under pressure, as revealed by in situ X-ray diffraction (XRD) on samples pressurized in diamond anvil cells.

Plutonium atoms are arranged, at ambient conditions, according to complex packing described by an unusual low-symmetry structure (monoclinic structure) with 16 atoms per unit-cell. This is the alpha (α)-phase. Alloying plutonium with aluminum, americium, cerium, or gallium stabilizes at room temperature the delta (δ)-phase of plutonium (a face-centered cubic structure with four atoms per unit-cell), but the detailed mechanisms at the origin of this phase stability or of the related phase transformations are still lacking. Furthermore, the δ-phase remains a great challenge for physicists to describe because of the complexity of its electronic structure, which results from a competition between itinerancy and localization in plutonium 5f states.

An example of XRD diagrams for the plutonium-2.3 at.% gallium alloy as a function of pressure and at room temperature. Analysis with the Rietveld method evidences the γ′-phase as an intermediate phase during the phase transformation.

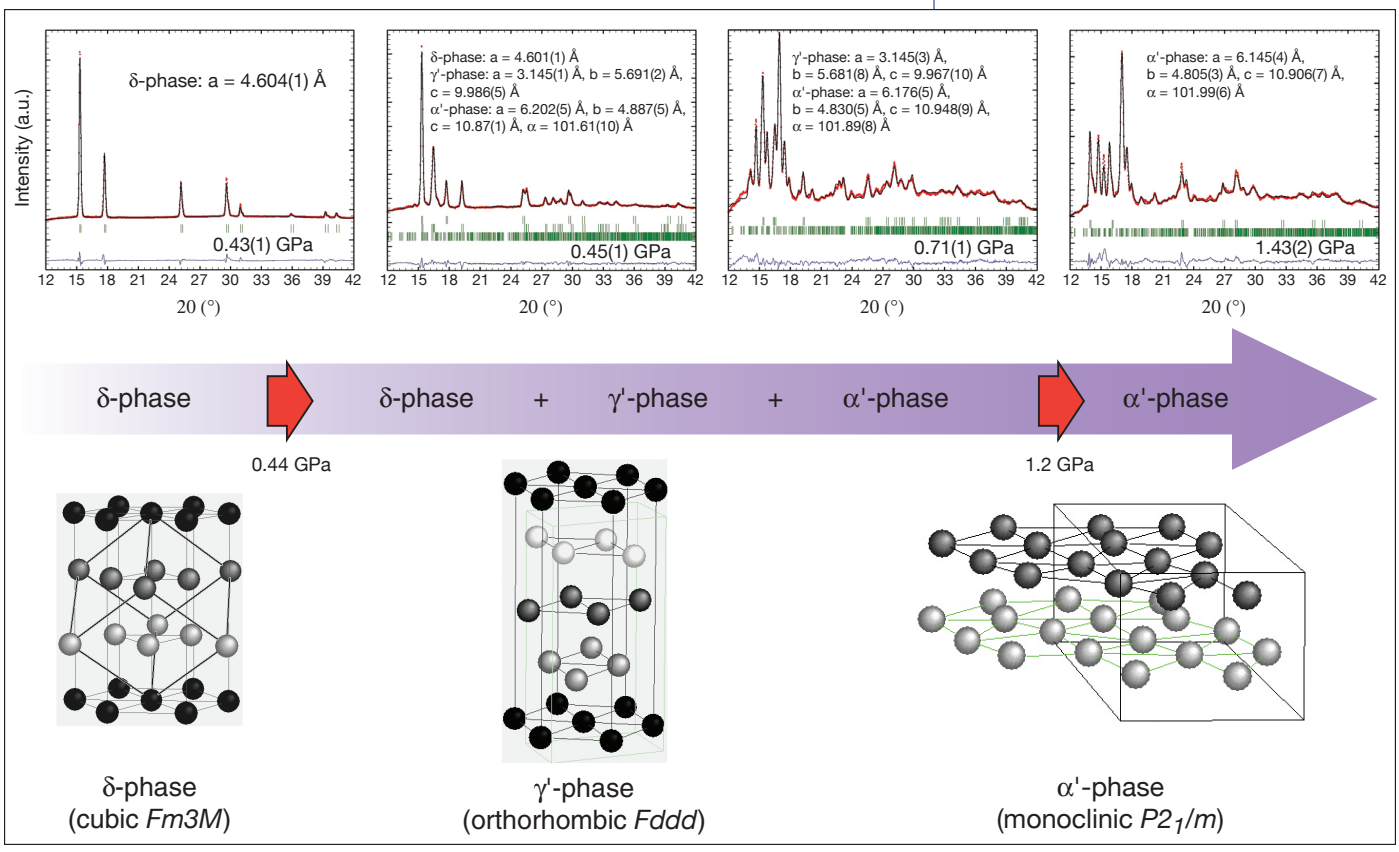

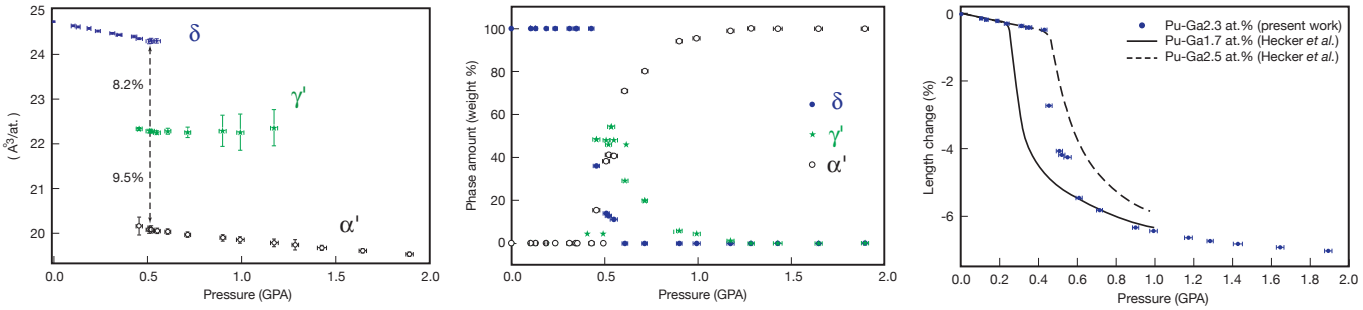

From left to right: Atomic volumes as a function of pressure for plutonium-2.3 at.% gallium, phase quantification for plutonium-2.3 at.% gallium, and length changes as a function of pressure. Data for plutonium-2.3 at.% gallium were calculated from XRD measurements while data for plutonium-1.7 at.% gallium and plutonium-2.5 at.% gallium were measured with a Bridgman-type pressure dilatometer (from S. Hecker et al.,* Progress in Materials Science *49, 2004).

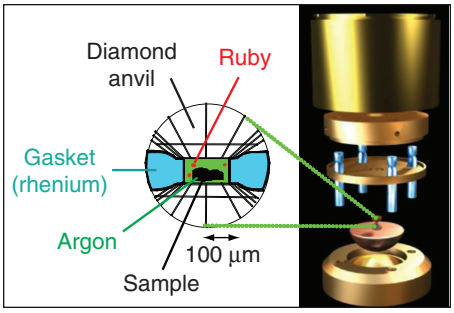

The diamond anvil cell used for the current study. The sample, about 100 µm long and 20 µm thick, is embedded in argon, a pressure-transmitting medium. Pressure is determined from the fluorescence of ruby spheres.

The delta-to-alpha prime (δ→α') phase transformation (the prime denotes solute atoms trapped in the a lattice) in δ-stabilized alloys can be triggered either by increasing pressure or by lowering temperature. Progress is being made in its description, but given the variety of behaviors (based on such parameters as solute type, solute distribution, impurities, and kinetics), additional experiments are required for a better understanding.

XRD is a particularly powerful technique because it provides direct evidence of the nature of the phases, the size of the corresponding unit-cell (and therefore interatomic distances and crystallographic anisotropy), and the amount of individual phases in mixtures. Coupling XRD with a diamond anvil cell allows the investigation of phase diagrams of materials over a wide range of pressure and temperature. This is why the technique is often used for determining equation of states (the relation linking, for instance, atomic volumes to pressure and temperature).

High-flux X-ray beams, as delivered by synchrotrons, are essential in experiments where very high pressures are required because the sample size must then be smaller than a few tenths of a micrometer (µm). But for moderate pressures—lower than about 50 gigapascals (GPa)—laboratory X-ray sources, such as the rotating anode, can also provide very good data.

XRD measurements on a plutonium-gallium alloy (Pu-2.3 at.%Ga) under pressure revealed clearly that the δ→α' phase transformation is indirect because it involves an intermediate phase—the gamma prime (γ')-phase (a face-centered orthorhombic structure with eight atoms per unit cell, similar to γ-plutonium but with solute atoms trapped in the lattice). Therefore, two to three phases coexist between 0.44(2) GPa and 1.2(1) GPa: the δ-phase, the γ'-phase, and the α'-phase. This result raises the question about the exact nature of this pressure-induced structural transformation and in particular regarding its martensitic character, the transformation being a two-stage transformation: δ→γ'→α'.

Plotting atomic volumes as a function of pressure reveals large volume collapses between δ and γ' phases (8.2%) and between γ' and α' phases (9.5%). The huge volume shrinkages may be linked to sudden pressure-induced delocalization of 5f electrons and a subsequent increase of the 5f electron participation in the metallic bonding. Such structural transitions should imply large stresses within the sample. These stresses may be at the origin of the slight increase of the γ'-phase volume observed while pressure is increased at the end of the transformation.

Knowing, for each phase, the phase amount and the corresponding atomic volumes, length changes can be calculated as a function of pressure. The resulting curve agrees qualitatively with dilatation measurements of Sig Hecker on homogenized Pu-1.7 at.%Ga and Pu-2.5 at.%Ga (in particular the compression before transformation and the shape and the magnitude of the curves during phase transformation). This data indicates that microscopic/atomic scale length changes derived from XRD yield the major behavior measured at a macroscopic level. It is not possible from such a continuous length change to guess that an intermediate phase occurs during the transformation. This proves why in situ phase characterization by XRD is essential to improving the understanding of such complex transformation.

The quantitative differences observed between XRD data and dilatation measurements may originate from experimental differences (such as kinetics, segregation, grain size, and eventual presence of non-diffracting impurities or phases) or from the XRD phase quantification accuracy. It would be very valuable, when possible, to perform such comparisons (microscopic information/ macroscopic measurements) that yield a global view of the system.

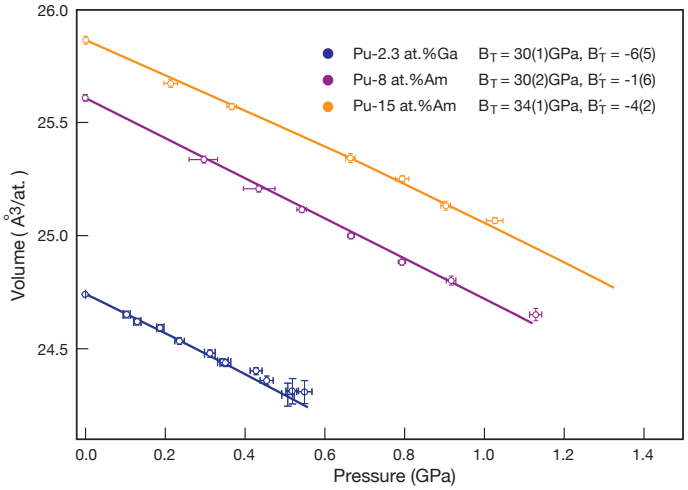

Atomic volumes as a function of pressure for several δ-stabilized plutonium alloys that present a softening under pressure. Continuous lines represent equation-of-state refinements. Plutonium-americium data are from P. Faure et al.,* Materials Research Society Proceedings *893, 2006, and V. Klosek et al.,* Journal of Physics: Condensed Matter *20, 2008.

When analyzing δ-phase atomic volumes, another anomalous property arises: the alloy softens under pressure (the first derivative with pressure, B'_T, of the isothermal bulk modulus, B_T, is negative). This property was predicted by the statistical mechanical model proposed by A.C. Lawson and others, based on a two-level "Invar"-like electronic structure, to account for δ-phase unusual thermodynamic properties measured at ambient pressure (for instance, a very small or even negative thermal expansion and a large elastic stiffness decrease with temperature). Consistency between different physical properties is thus obtained for the δ-phase.

Further reading:

Challenges in Plutonium Science I and II, *Los Alamos Science,* Volume 26, 2000.

"Invar Model for δ-Phase Pu: Thermal Expansion, Elastic and Magnetic Properties," A.C. Lawson et al., *Philosophical Magazine* 86, Issues 17 & 18, June 2006.

Actinide Hydration, Hydrolysis, and Aggregation

This article was contributed by Lynne Soderholm, Richard Wilson, and Suntharalingam Skanthakumar, Chemical Sciences and Engineering Division, Argonne National Laboratory.

At right: A representative thorium dimer crystal, measuring 200 x 70 µm, is mounted on the end of a glass fiber and ready for structural determination.

The synthesis and characterization of actinide oligomers, aggregates, and nanoparticles formed the basis for this plenary lecture from the group at Argonne National Laboratory. The presentation centered on demonstrating the mechanisms by which hydrolyzed tetravalent actinide ions condense in aqueous solutions and their impacts on product formation.

The talk began with a review of the two mechanisms typically used to account for metal-ion condensation in aqueous solution. The first mechanism is the olation reaction, which involves the formation of hydroxo-bridged, poorly defined amorphous oxyhydroxides. The second mechanism is the oxolation reaction, which produces oxo-bridged species with chemically and structurally well-defined clusters, such as the polyoxometalates formed with high-valent transition-metal oxides. The tetravalent actinides are traditionally thought to be soft enough that their condensation can been viewed within the olation scheme and the products assessed as amorphous and chemically poorly defined.

The discussion of experimental results began with a description of some thorium (Th^{4+}) hydrolysis products with a note that thorium is the softest tetravalent ion. High-energy X-ray scattering (HEXS) data obtained from solution show evidence of oligomerization, a finding corroborated by structural determinations of crystals obtained from the same solutions. Unequivocal evidence was provided of hydroxo-bridged dimers, consistent with expectation. Interesting to note were the HEXS data obtained from cloudy, aged, thorium solutions showing evidence of thorium–thorium correlations consistent with oxo-bridged moieties.

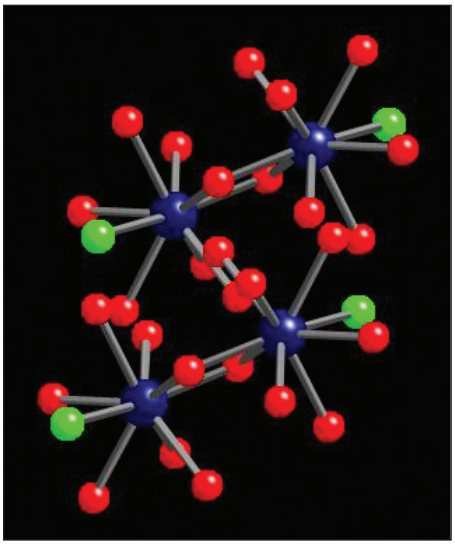

Hydroxyl-bridged thorium dimers, with each thorium also bound to five waters and a terminal chloride (green) determined by X-ray single-crystal structural analysis. The presence of the bridged thorium species in solution is confirmed by HEXS.

The results from similar experiments on plutonium (Pu^{4+}) hydrolysis were markedly different. The solutions, which showed behavior consistent with plutonium polymer, produced HEXS patterns interpretable as arising from monodisperse solutions of PuO_2-based nanoparticles (see figure at right). X-ray diffraction structural analyses on crystals obtained from these solutions are consistent with this interpretation, with calculated HEXS patterns reproducing both the interatomic distances and the peak intensities.

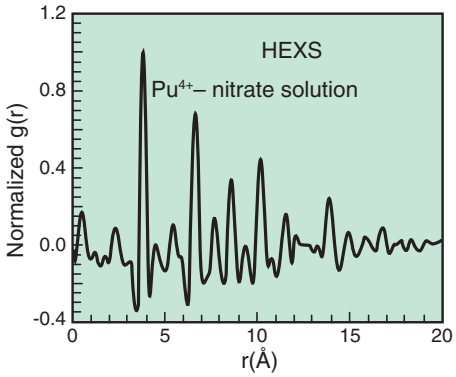

$[Pu_{38}O_{56}Cl_{54}(H_2O)_8]^{14-}$ was chosen as a representative cluster for further description. At its core is a plutonium-oxygen aggregate with a structure only slightly distorted from the Fm3m symmetry expected for PuO_2. There is no evidence of any OH^- or other defect ions within the moiety itself. The cluster core, with a charge of +40, is decorated on the outside with both waters and in this case chloride, which brings the overall cluster charge down to -14. It is unclear from the HEXS data whether all the chlorides remain on the cluster surface in solution. Several similar structures have been determined. The Pu-O cluster core remains relatively invariant but the number, type, and nature of the decorating anions are subject to change.

Crystals with several other Pu-O cluster sizes were also reported, some of which involved surface-complexed anions other than chloride. HEXS data combined with the structural results suggest that the size of the metal-oxide cluster depends somewhat on the dissolved anions in solution. Optical spectra from a variety of different solutions were shown suggesting that the anions decorating the clusters are labile and can be replaced by changing solution conditions without altering the metal-oxide core, once it is formed.

Overall, the work has several implications, the most important of which points to an oxolation mechanism for the condensation of hydrolyzed Pu^{4+}, in contrast to the olation mechanism seen for Th^{4+}. The determination that plutonium hydrolysis results in chemically and structurally well-defined large PuO_2-based nanoclusters, combined with the lability of surface-ligated anions, suggests a new approach to predicting and controlling the plutonium chemistry relevant to current separations and environmental issues.

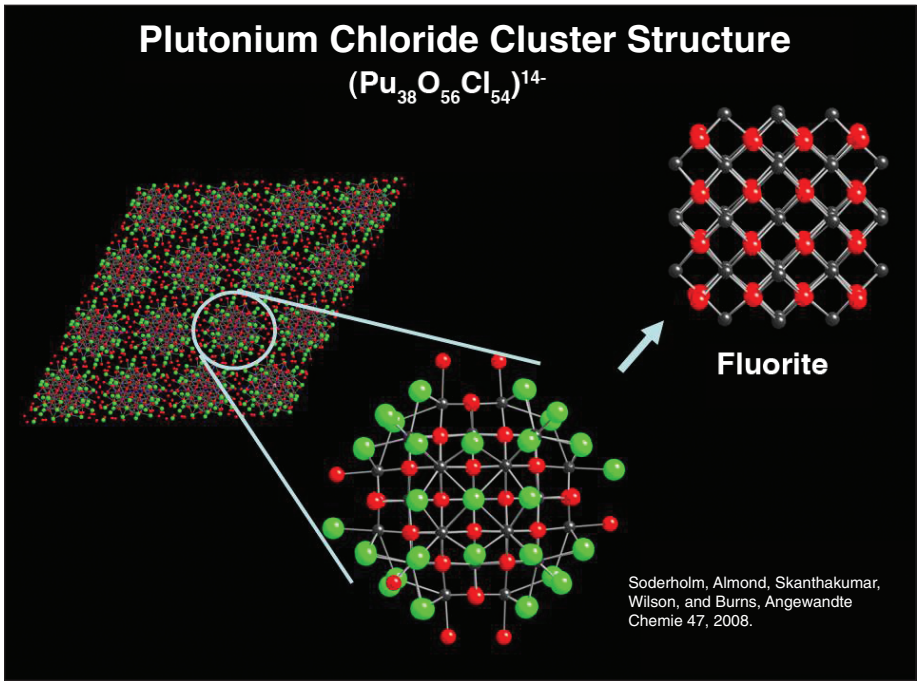

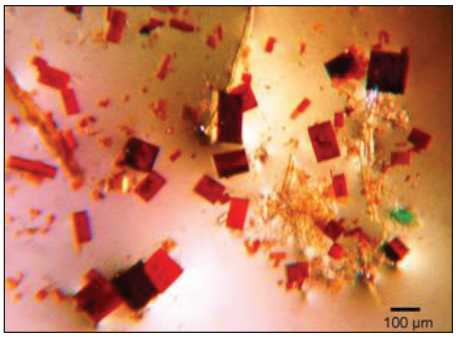

Single crystals of the plutonium-38 clusters, which appear red in their predominant motif. The green crystal represents another motif of similar material.

This work is supported at Argonne National Laboratory by the DOE Office of Basic Energy Sciences/Chemical Sciences under contract DE-AC02-06CH11357.

This article was contributed by David Pugmire, Harry Garcia Flores, David Moore, Charles Davis, and Amanda Broach, Materials Science and Technology Division, Los Alamos National Laboratory.

The Role of Gallium During the Oxidation of δ-Stabilized Plutonium

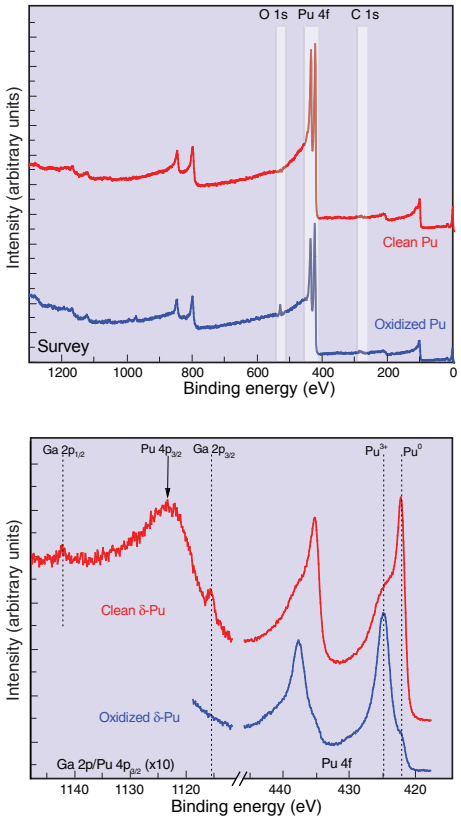

XPS data for a clean plutonium sample (red) and the same sample after controlled oxidation with water (blue) are shown in the top figure. The peak in the O 1s region (blue) indicates a marked increase in the oxygen content upon oxidation. The figure above shows high-resolution XPS data for the plutonium 4f (right) and gallium 2p (left) regions. The small peaks indicated by the dotted lines in the gallium 2p spectrum on the left indicate that gallium is observed at the surface of the clean plutonium metal.

The oxidation of plutonium has been studied almost since the discovery of the element. The oxidation characteristics and rates for plutonium have significant implications for production use, storage, and disposition of this reactive metal. It has been shown that the rate of oxidation for the delta (δ)-phase stabilized, gallium alloy can be significantly slower than that for unalloyed plutonium. The reason for the rate change upon alloying with gallium is not understood.

A previous study of a variety of δ-stabilized plutonium alloys shows that the significant structure difference between unalloyed alpha (α)-phase plutonium and alloyed δ-plutonium cannot be the sole cause of different oxidation rates. These facts imply that the alloying metal must play some role in the slower oxidation rates observed for gallium-stabilized δ-plutonium. Therefore, to elucidate the oxidation mechanism of this commonly employed alloy, it is important to understand the role gallium plays during oxidation.

The relatively low concentrations of alloying metals used, typically several atomic percent (at.%), can make the activities of gallium during oxidation of δ-plutonium difficult to follow. This complication is compounded by the fact that the initial stages of oxidation are inherently a surface phenomenon, thereby significantly limiting the relative amount of affected material. An ultrahigh vacuum (UHV) system equipped with surface-sensitive techniques, such as X-ray photoelectron spectroscopy (XPS) and Auger electron spectroscopy (AES), provides a controlled environment ideally suited to study the oxidation of surfaces.

AES analysis is ideally suited to be coupled with an ion-milling technique (such as argon ion sputtering) to perform depth profiles that consist of elemental composition data as a function of sputter depth into a sample. This method has been employed at Los Alamos to estimate the thickness of the oxide films. While some surface-science techniques suffer from relatively high limits of detection, we have been able to qualitatively study the behavior of gallium during the oxidation of the δ-stabilized plutonium alloy with XPS and AES.

We have also studied this system using electron-probe microanalysis (EPMA), which does not suffer from the same high limits of detection. As with depth profiling, EPMA may also provide some information about variations in sample composition with depth by varying the incident electron-beam accelerating voltage. Depth of analysis varied from approximately 120 nanometers (nm) at 5 kilovolts (kV) to approximately 500 nm at 15 kV.

X-ray photoelectron spectroscopy was used to study a clean (argon ion etched) plutonium sample and the same sample after controlled oxidation with water. As expected, the data indicate a marked increase in the oxygen content at the surface upon oxidation. Corresponding high-resolution XPS data for

the plutonium 4f and gallium 2p regions indicate that the majority of the plutonium at the surface of the clean sample is metal (Pu^0). Upon oxidation, a spectrum showing a majority of the plutonium at a binding energy consistent with the +3 state (Pu^{3+}, Pu_2O_3) is observed. Corresponding gallium 2p data indicate that gallium is observed at the surface of the clean plutonium metal. The gallium $2p_{3/2}$ region for the sample after oxidation indicates that the relative gallium concentration at the surface has decreased to the point that it is no longer observed.

The conclusion, as may be drawn from the XPS data, that gallium is removed or depleted from the near-surface region during the oxidation of δ-stabilized plutonium, is also observed in electron microprobe data of oxide films of varying thickness. The microprobe data for a thin oxide film (estimated to be 30 nm thick) yield a gallium concentration of approximately 2.0 at.% as expected, based on the bulk concentration for this sample. The data for the thickest film studied (approximately 300 nm), show an approximate value for the gallium concentration of 0.6 at.%, significantly lower than what was observed for the thin oxide film, and are expected for the bulk of this sample. The data from the 30- and 300-nm films yield gallium concentrations that do not vary significantly with depth (i.e., accelerating voltage).

A much different result is obtained from films of intermediate thickness. The data from a gallium concentration for an approximately 100-nm-thick oxide film show that at lower accelerating voltages, the gallium concentration is closer to that observed for the thick oxide, and as the accelerating voltage is increased, the concentration increases, approaching the expected bulk value at 15 kV. Modeling of this data indicates that only a system in which the gallium content is significantly reduced in the oxide film will qualitatively yield these results.

In an Auger depth-profile through an approximately 300-nm oxidized plutonium film, it is possible to differentiate between the Auger signal originating from oxidized plutonium atoms and that of plutonium metal atoms. The data show that the relative concentrations as a function of depth for the oxidized plutonium species and the oxygen species follow each other, both dropping significantly in concentration by 300 nm. A plutonium metal signal is observed as early as approximately 75 nm into the oxidized plutonium film. The data also show that the gallium concentration is below the limit of detection at the surface of the film, but begins to appear at the same depth as the first observation of signal due to plutonium metal.

Initially, the increase in the gallium concentration follows the observed increase for the plutonium metal concentration. However, at approximately 200-nm depth, this trend abruptly changes. Between 200 and 300 nm, a new gallium/plutonium metal relative concentration is established and appears to hold to 900 nm depth (through the oxide film and indicative of the bulk metal). The gallium/plutonium metal concentration ratio observed for the "bulk" with Auger depth-profiling is significantly low, at a value of 0.7% (as opposed to the expected value of 2.0%). This is likely due to preferential sputtering (i.e.,

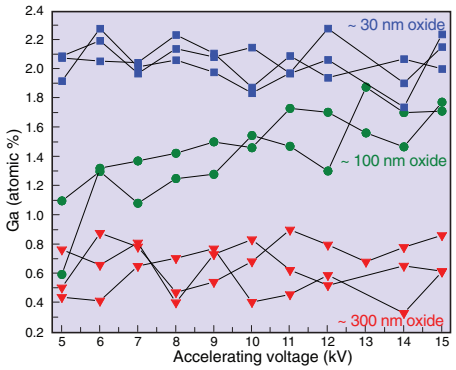

Electron microprobe data of oxide films of varying thickness. This figure shows the observed gallium concentration (atomic percent) as a function of electron-beam accelerating voltage for oxide films grown on a sample with 2.0 at.% gallium content. Multiple data points at each accelerating voltage show results from several different locations across each sample/film surface (data from each location are connected with a line).

Further reading:

"Atmospheric Corrosion Tests of Several Delta Phase Alloys of Plutonium," J.T. Waber et al., *Journal of Nuclear Materials* 3, 1961.

Plutonium Handbook, O.J. Wick, editor, American Nuclear Society, La Grange Park, Illinois, 1980.

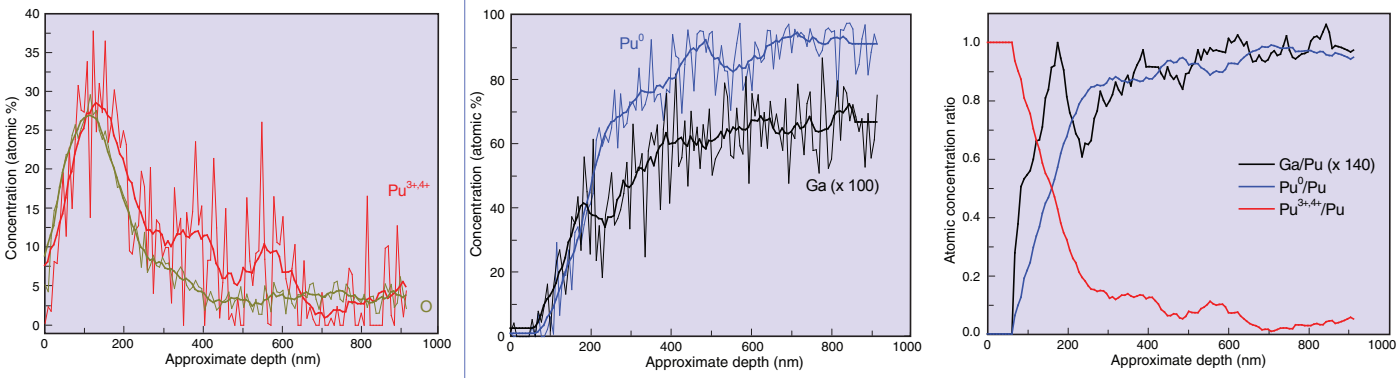

Auger depth-profile through the ~300 nm oxidized plutonium film. It is possible to differentiate between the Auger signal originating from oxidized plutonium atoms and that of plutonium metal atoms, as indicated by the separate traces shown for "$Pu^{3+,4+}$" and "Pu^0" in the figures at left and center, respectively. The figure on the left shows that the relative concentrations as a function of depth for the oxidized plutonium species and the oxygen species follow each other, both dropping significantly in concentration by 300 nm. As shown in the figure in the center, plutonium metal signal is observed as early as ~75 nm into the oxidized plutonium film. This figure also shows that the gallium concentration is below the limit of detection at the surface of the film but begins to appear at the same depth as the first observation of signal due to plutonium metal (the gallium concentration trace has been multiplied by 100 in the center figure). The figure on the right shows the plutonium metal, oxidized plutonium, and gallium concentrations normalized to the total plutonium concentration as a function of sputter depth. This figure further highlights the features observed in the center figure, mainly that there are three distinctly different regions in the gallium depth profile.

preferential removal of lighter atoms), as has been seen previously for many multielement systems.

When the plutonium metal, oxidized plutonium, and gallium concentrations are normalized to the total plutonium concentration as a function of sputter depth, the data highlight the features that there are three distinctly different regions in the gallium depth profile: (1) the first approximately 75 nm of the film, in which gallium is not observed; (2) beginning near the oxide/metal interface and continuing into the metal (greater than 250 nm) where a constant gallium-to-plutonium ratio is established, expected to be representative of the bulk gallium concentration; and (3) an intermediate region (approximately 75–200 nm) in which the relative gallium concentration appears to be enriched.

The data obtained thus far for the room-temperature oxidation of gallium-stabilized δ-plutonium indicate that the gallium concentration is significantly depleted at the surface and within the oxide film. XPS data show the disappearance of gallium at a clean metal surface upon oxidation. Thicker oxide films grown in air show depletion of the gallium concentration in the near-surface region, as indicated by electron microprobe data. Auger depth-profiles of oxide films on plutonium indicate the presence of a gallium-depleted region at the surface and a gallium-rich region at the oxide/metal interface.

A gallium-depleted oxide film on δ-stabilized plutonium would have very similar elemental composition to an oxide film on unalloyed α-plutonium and would be expected to have little or no effect on the comparative oxidation rates. Therefore, it is very likely that the mechanism for the reduction of plutonium oxidation rates upon alloying with gallium is related to the corresponding enrichment at the oxide/metal interface. A thin, gallium-rich (and therefore plutonium-poor) region at the oxide-metal interface could significantly reduce the number of plutonium atoms available for reaction with oxygen, thereby slowing the oxidation rate as the oxide film increases in thickness.

A LINK BETWEEN THE OXIDATION STATES?

COLLOIDS AND MIXED-VALENCE POLYMERS OF PLUTONIUM IN AQUEOUS SOLUTION

This article was contributed by Clemens Walther, Jörg Rothe, Markus Fuss, and Sebastian Büchner, Institut für Nukleare Entsorgung (INE), Forschungszentrum Karlsruhe.

Soon after production of the first micrograms of plutonium in the 1940s, the high tendency of tetravalent plutonium to form polymeric complexes and colloids became obvious. "Plutonium people" have been struggling with these mostly unwanted species ever since. Due to the complexity of plutonium chemistry, the exact processes underlying polymer and colloid formation are still controversial.

We use the term colloids to describe polymers large enough to be detected by laser-induced breakdown detection (LIBD), i.e., larger than approximately 5 nanometers (nm) in diameter. In our current study, we aim to understand the formation mechanisms by combining modern state-of-the-art analytical techniques.

We prepared aqueous solutions ranging from [Pu(IV)] = $2x10^{-6}$ moles per liter (mol/L) to 10^{-3} mol/L and pH_C 0–2.1 and investigated them by different methods. From extended X-ray absorption fine structure (EXAFS) data taken in the millimolar concentration range, we concluded that polymerization of tetravalent plutonium proceeds via aggregation of cubic plutonium-dihydroxo building blocks [$Pu(OH)_2^{2+} \cdot 6H_2O$] followed by partial condensation $2OH^- \leftrightarrow H_2O + O^{2-}$, leading to the formation of larger moieties such as dimers, trimers, and so on.

Artist's view of the electrospray process. The nanometer-sized charged droplets emanating from the nano ESI capillary become visible by light scattering of a counter propagating laser beam. These droplets evaporate solvent and shrink in size until single polymers with a small solvent shell remain. These are analyzed by time-of-flight mass spectrometry.

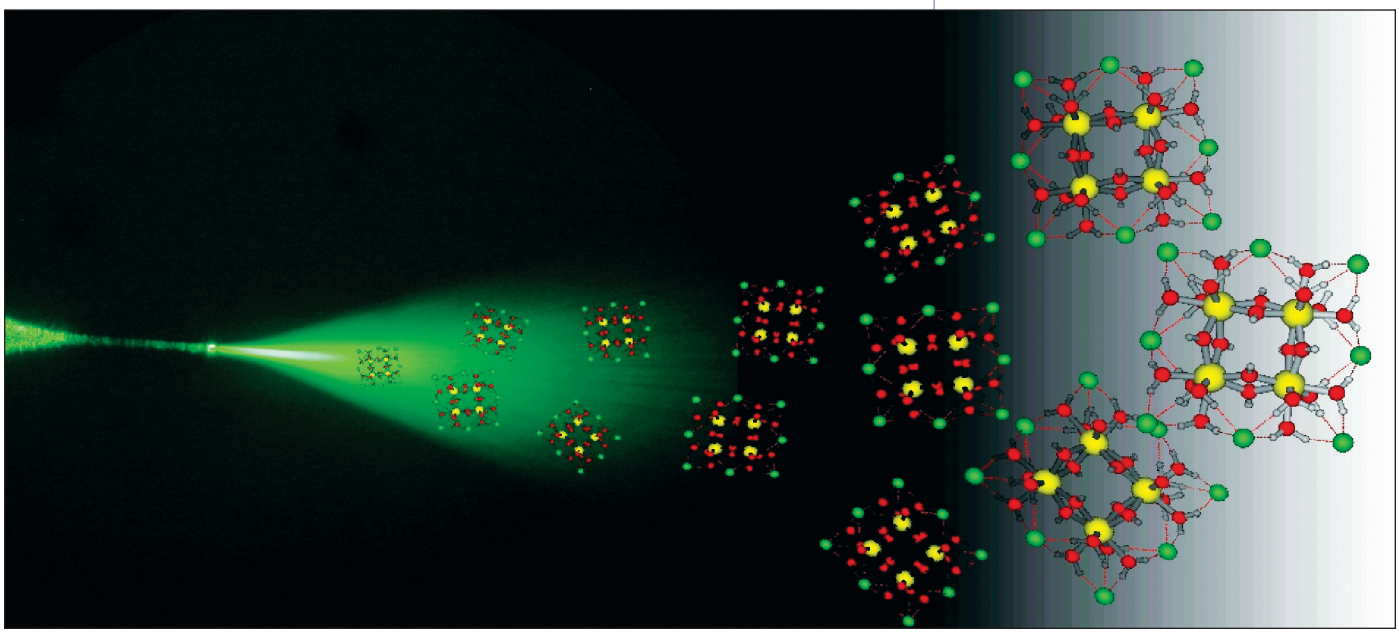

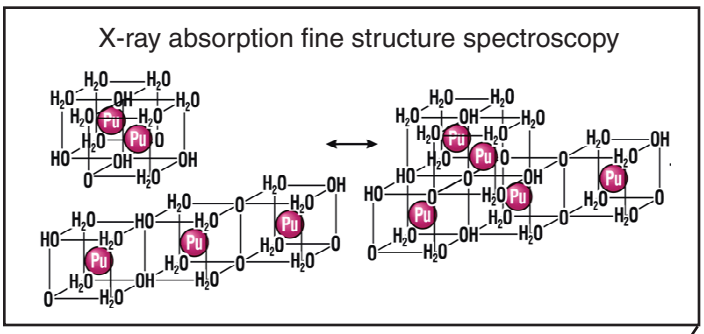

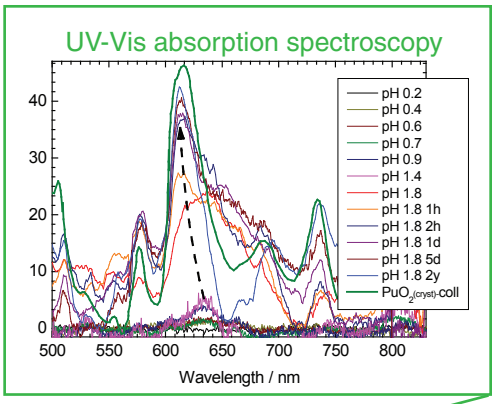

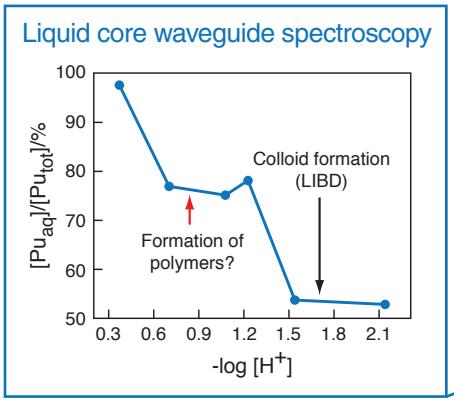

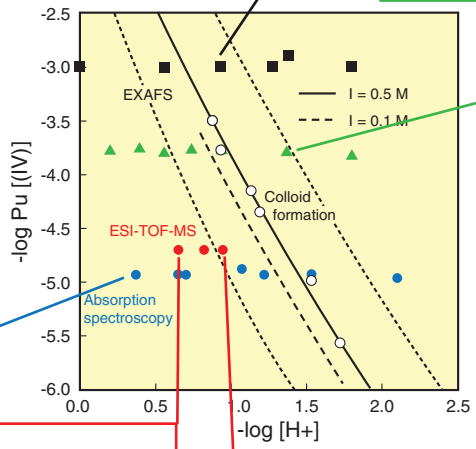

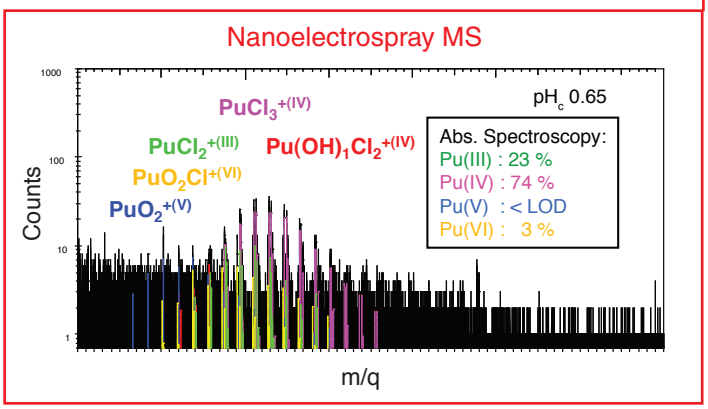

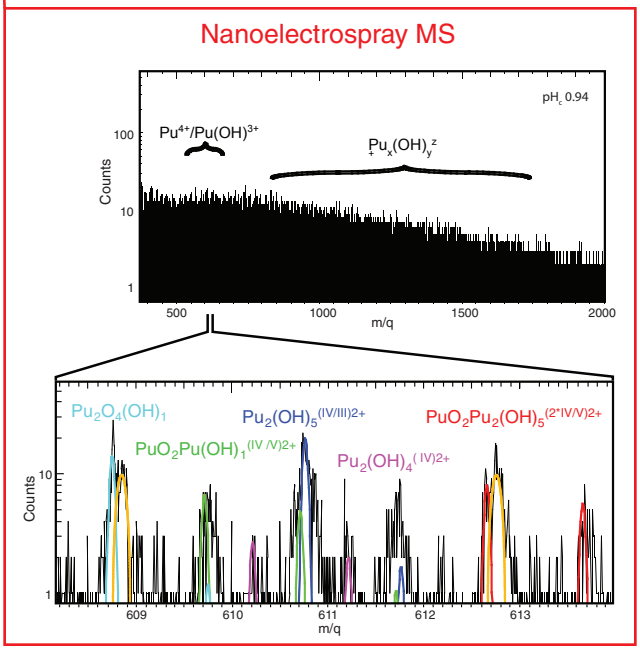

Acidic Pu(IV) solutions are investigated by different techniques. Based on EXAFS measurements, the polymerization process of Pu(IV) is modeled by stacking of cubic $Pu(OH)_2^{2+}$ units (black box). Aging of colloids leads to a change in visible absorption spectra (green box). The formation of small polymers causes a decrease in absorption of the Pu_{aq}(tot) absorption and is directly observed by ESI TOF MS. Of particular relevance is the formation of mixed-valence polymers that contain Pu(III) or Pu(V) in addition to Pu(IV).

Due to nonperfect stacking, the resulting structure exhibits a disturbed Pu-O-Pu backbone with increasing order as the size increases. The Pu-O coordination shell shows a variable degree of order due to the variation in numbers of O^{2-}, OH^-, and H_2O ligands in the growing structural network. These fresh, disordered colloids (often denominated amorphous oxo-hydroxide colloids) undergo a ripening toward a face-centered-cubic PuO_2 structure. We observed this process by optical absorption spectroscopy.

Polymerization was induced in a sample at [Pu(IV)] = $2x10^{-4}$mol/L by stepwise pH increase, as evident from the increasing signal around λ = 630 nm. After reaching pH_C 1.8, the sample was allowed to age for two years. During this time the absorption peak increased further, shifted to shorter wavelengths, and finally closely resembled the well known absorption spectrum of crystalline PuO_2 colloids observed in concentrated plutonium solutions by Richard Haire of Oak Ridge National Laboratory.

Whereas aged Pu(IV) colloids are close to insoluble, fresh colloids and polymers are in equilibrium with monomeric ionic solution species. Thus, a complete understanding of the complex redox chemistry of plutonium is not possible without including colloids. (See "Solubility and redox equilibria of plutonium," Thomas Fanghänel, *Actinide Research Quarterly,* 3rd/4th Quarters, 2006.)

Typical green color of a concentrated solution containing Pu(IV) colloids.

The Pu(III)/Pu(IV) couple as well as the Pu(V)/Pu(VI) couple equilibrate quickly, but oxidation of the tetravalent ion $Pu(IV)_{aq}$ to the trans-dioxo species PuO_2^+ [Pu(V)] is very slow. Thomas Newton, a former member of Los Alamos National Laboratory, reported that the inverse process—the reduction of Pu(V)—does not occur in the absence of "Pu(IV) colloids."

To gain insight into the mechanisms of colloid formation on a molecular level, we prepared solutions close to the solubility limit of amorphous plutonium hydroxide at concentrations below 10^{-4} mol/L. To avoid oversaturation, we monitored colloid formation by means of LIBD. This technique is capable of measuring the size distribution of inorganic aquatic colloids larger than approximately 5 nm at low concentration and gives very precise solubility data. The formation of colloids as detected by LIBD coincides with a decrease in optical absorption of the Pu(IV) band at 471 nm measured by a very sensitive type of UV-Vis spectrometer, the liquid core waveguide capillary cell with a 1-meter path length. However, yet another decrease was observed at considerably lower pH, which cannot be attributed to the formation of colloids. We suspected formation of weakly absorbing polymers to be responsible.

Direct proof was obtained by using nanoelectrospray time-of-flight mass spectrometery (ESI TOF MS), operated in the soft mode, leaving the molecular ions in an intact solvent shell of some 50 water molecules while still allowing us to determine the mass-over-charge ratio to high precision (typically $m/\Delta m$ = 15000). From this data, the number of plutonium ions (in this case plutonium-244), OH^- ligands, Cl^- counterions, water adducts, and the overall charge of the complex of molecules were obtained.

At pH_C 0.65, which is undersaturated by a factor of >50, only the mononuclear ions Pu^{3+}, Pu^{4+}, $Pu(OH)^{3+}$, PuO_2^+, and PuO_2^{2+} appeared in the mass spectrum. Their relative abundances are in good accordance with the distribution obtained by absorption spectroscopy. A slight decrease of the acidity to pH_C 0.94 (undersaturation ~10) resulted in a much richer mass spectrum extending to higher masses. In contrast to analogue experiments on thorium(IV) and zirconium(IV), however, the spectra could not be fitted by including $M_x^{(IV)}(OH)_y^{z+}$ polymers alone. Instead, a great variety of polymers were identified where Pu(IV) was partly substituted by Pu(III), or Pu(V) (so-called mixed polymers). In the magnified section of the spectrum some dimers and trimers are annotated exemplarily, omitting the counterions (Cl^-) and water adducts for clarity. The full spectrum is identified by including close to 50 different species, each with a distribution of water adducts ranging from approximately 20 to approximately 80, which totals some 3000 peaks.

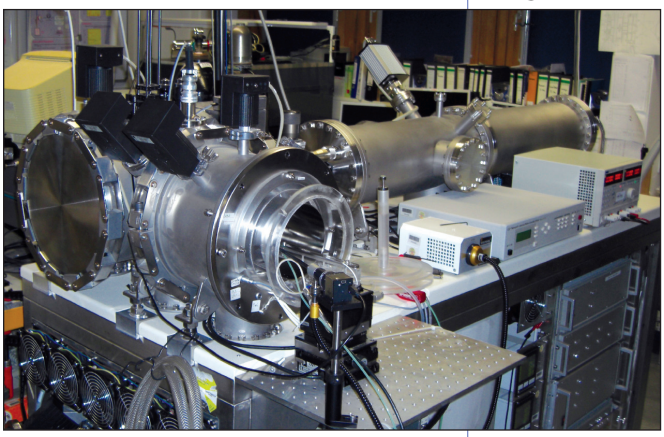

The high-resolution time-of-flight mass spectrometer (BME Albatros) with home-built nanoelectrospray source used for our current study.

In particular, the polymers containing both Pu(IV) and PuO_2^+ are of great interest because they might present the long-looked-for transition species during oxidation from Pu(III)/Pu(IV) to the trans-dioxo ions PuO_2^+ and PuO_2^{2+} and reduction of Pu(V)/Pu(VI), respectively, even in dilute solutions in the absence of colloids or precipitates.

Their role would explain Newton's finding that reduction of Pu(V) is strongly hindered in the absence of colloids, and may also be important in the formation process of the overstoichiometric PuO_{2+x} solid. Furthermore, since colloids most likely form by aggregation and growth of plutonium-hydroxide colloids, the observation of a very short Pu-O distance in EXAFS spectra of concentrated colloidal plutonium suspensions (which was interpreted by Steven Conradson and David L. Clark of Los Alamos in terms of the presence of PuO_2^+) corroborates the present finding.

PLUTONIUM: THE DENSITY-FUNCTIONAL THEORY POINT OF VIEW

This article was contributed by Per Söderlind and Alex Landa of Lawrence Livermore National Laboratory.

Density-functional theory (DFT) is a remarkably successful tool for describing many metals throughout the Periodic Table. Here we present the results of this theory when applied to plutonium metal, perhaps the most complex and difficult-to-model metal of all.

The fundamental product of DFT is the ground-state total energy. In the case of plutonium, we show that DFT produces total energies that can predict the complex phase diagram accurately. Focusing on the delta (δ) phase, we show that DFT electronic structure is consistent with measured photoemission spectra. The observed nonmagnetic state of δ-plutonium could possibly be explained in DFT by spin moments, likely disordered, that are magnetically neutralized by antiparallel aligned orbital moments. As an alternative to this nonmagnetic model, an extension of DFT with an enhanced orbital polarization is presented in which magnetism is suppressed.

Plutonium metal has many physical properties that are counterintuitive, puzzling, and intriguing. The most perplexing behaviors of plutonium are displayed in its phase diagram: it has as many as six condensed phases with stark contrasts in both atomic geometry and volume. At lower temperatures, plutonium has very low symmetry atomic arrangements with small volumes (α and β monoclinic), then with increasing temperature it expands to higher symmetry (γ orthorhombic and δ cubic), followed by a volume collapse to lower symmetry (δ′ tetragonal) before shrinking (ε cubic).

These transitions take place in a limited temperature range, suggesting that the phases compete closely with each other. Plutonium thus provides an extraordinary challenge for any theory that describes phase stability. In the literature one finds several models for plutonium that unfortunately cannot be discussed in this short article.

The foundation of modern DFT took shape in the mid 1960s with the papers by Pierre Hohenberg and Walther Kohn and Kohn and Lu J. Sham, for which Kohn received the Nobel Prize in Chemistry in 1998. The theoretical framework has been implemented in gradually more accurate computer codes since its invention and is now the essential workhorse for first-principles calculations for materials. Although popular for describing many materials, its usefulness for

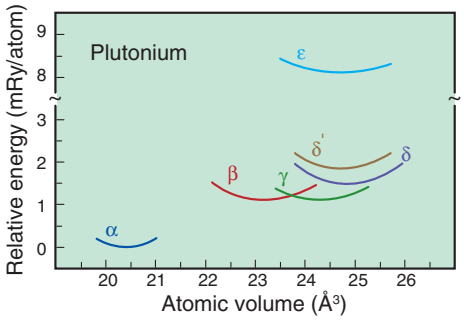

DFT total energies for the six known condensed phases of plutonium. The order of ranking for the total energies as well as the atomic volumes is the same in DFT as in the phase diagram.

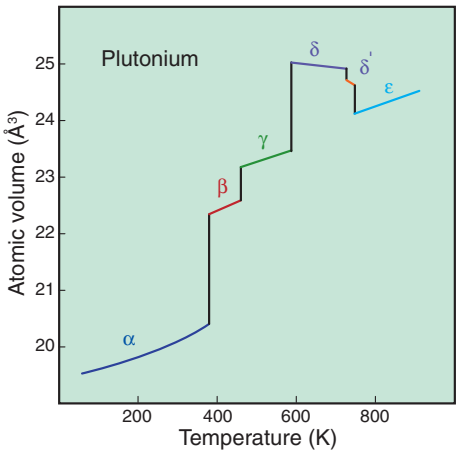

The experimental phase diagram of plutonium displays the metal's perplexing behaviors.

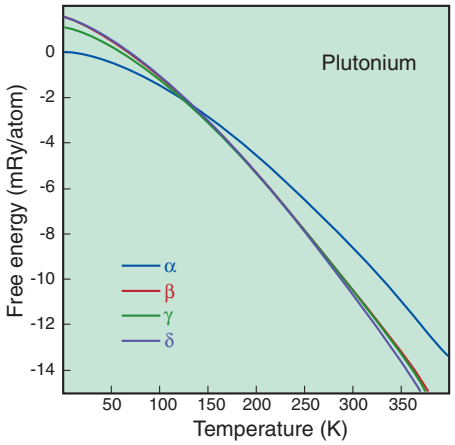

Helmholtz free energies. Because the various plutonium phases are all stable at relatively low temperatures, the DFT total energy can approximately be corrected for temperature (vibrating atoms) within a quasi-harmonic approach. The result of this correction is shown here by plotting the free energy as a function of temperature for the α, β, γ, and δ phases. The figure shows that temperature stabilizes these phases in accordance with the known phase diagram.

plutonium may have escaped some of the nonspecialists. Here we review some of the results and insights DFT gives us for plutonium.

One important challenge for any theory is to evaluate its capability to reproduce or predict a phase diagram. The word "predict" is appropriate for DFT because in this theory no adjustable parameters are used to reproduce a wanted (experimental) result. When we contrast DFT total energies for the six known phases of plutonium with the experimental phase diagram, the theory ranks the total energies in the order α, β, γ, δ, δ′, and ε. This exact order is also found in the experimental phase diagram as a function of temperature. In DFT, the atomic volumes order exactly the same way as in the experimental phase diagram. Hence, DFT captures the main features of the very delicate and complex phase diagram of plutonium.

Because the various plutonium phases are all stable at relatively low temperatures, the DFT total energy can approximately be corrected for temperature (vibrating atoms) within a quasi-harmonic approach. When we plot the free energy as a function of temperature for the α, β, γ, and δ phases, temperature stabilizes these phases in accordance with the known phase diagram. This is a testament to the high quality of the DFT total energies. Comparable results have been published elsewhere.

Next, we focus on the important δ phase and relate the theoretical electronic structure with measured data. When we plot calculated electronic density-of-states (DOS) that have been appropriately convoluted with instrumental and lifetime broadening, together with experimental photoemission data at two photon energies, the spectra are consistent with each other and DFT appears to agree with experiments for δ-plutonium.

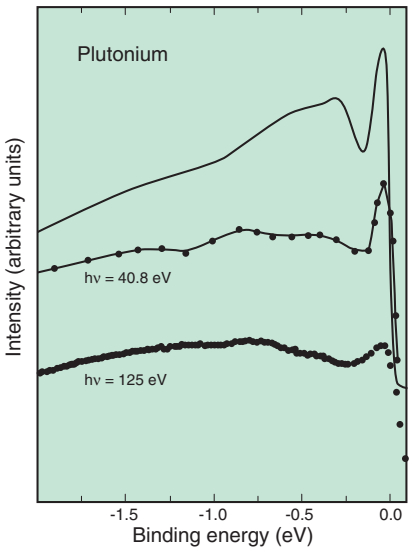

Experimental δ-plutonium photoemission spectra (125 eV and 40.8 eV) and theory. These spectra are consistent with each other, and DFT appears to agree with experiments for δ-plutonium.

The DFT electronic structure is spin polarized with a resulting spin moment on each plutonium atom. This would seem to imply that theory predicts δ-plutonium to be magnetic, something that has not been observed for pure plutonium metal. But for plutonium nothing is simple or intuitive. Examining

the DFT results for δ-plutonium, it has been realized that (1) at temperature where it is stable, the spins are most likely disordered and (2) the orbital moment may perfectly cancel the spin moment, making each plutonium atom magnetically neutral. If DFT is correct regarding (1) and (2), then it makes sense that no conclusive evidence of magnetism in δ-plutonium has been revealed.

If neither (1) nor (2) is correct, then it is likely DFT is insufficient in modeling the nature of magnetism in plutonium. It has been suggested that orbital correlations, in terms of spin-orbit coupling and orbital polarization, are much stronger than spin correlations, and therefore the spin moments could appropriately be suppressed in a constrained DFT treatment. When we plot the total energies for calculations with the spin moment quenched (NM) in combination with spin-orbit coupling (SO) and orbital polarization (OP), the addition of SO and OP lowers the total energy substantially while simultaneously expanding the metal closer to the observed volume (V_δ). Allowing ferromagnetic spin polarization lowers the total energy further but does not improve on the equilibrium volume.

It was further shown that the main features (peak locations) of the DOS did not depend sensitively on the spin restriction. Therefore, one can argue that suppressing the spin moment, when the mentioned orbital correlations are accounted for, is a reasonable nonspin DFT model for δ-plutonium. Another interesting observation is that SO and OP tend to quench the spin moment (from 5 μ_B to about 3 μ_B).

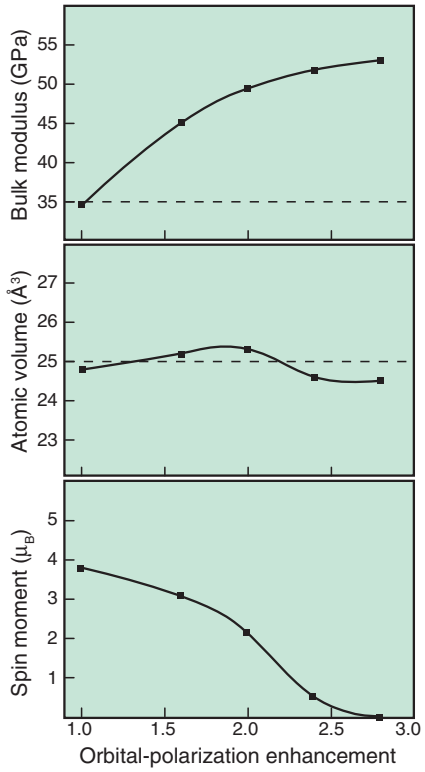

Spin (S), atomic volume (V), and bulk modulus (B) as functions of orbital-polarization enhancement factor. Dashed horizontal lines denote the measured values.

The fact that spin-orbit coupling and orbital polarization have an intricate relationship to the spin moment was recently reported by Francesco Cricchio et al. in *Physical Review B* (2008). By introducing two parameters, Cricchio was able to suppress the spin moment and accomplish a nonmagnetic state in δ-plutonium. In the article, "Exchange Energy Dominated by Large Orbital Spin-Currents in δ-Pu," Cricchio discussed that the "conventional" OP correction, as used here and introduced by M.S.S. Brooks in a paper published in *Physica B* (1985), could effectively be strengthened to possibly accomplish a similar nonmagnetic state for δ-plutonium.

Calculations for δ-plutonium were also done in the same fashion as the

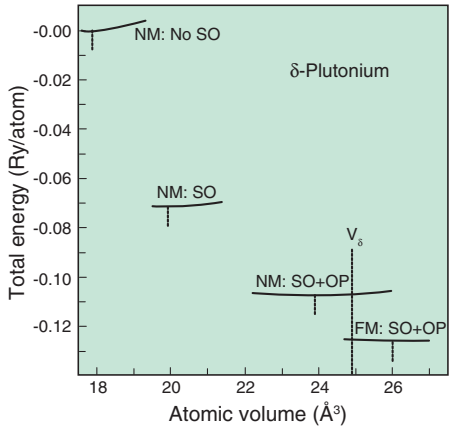

DFT total energies, nonmagnetic (NM, zero spin) and ferromagnetic (FM), for δ-plutonium. Spin-orbit interaction and orbital polarization are denoted SO and OP, respectively.

This work was performed by Lawrence Livermore National Laboratory under the auspices of the DOE under contract DE-AC52-07NA27344.

ones presented in the figure at the bottom of Page 23, but with an amplified OP. An amplification factor equal to unity corresponds to our standard OP, while a greater value attempts to model the full treatment with the introduced adjustable parameters. The ferromagnetic spin moment gradually approaches zero with increasing OP enhancement. At the same time, the atomic volume remains close to the observed value, whereas the bulk modulus apparently is becoming somewhat large. Thus, this approach, as well as the more complete treatment reported by Cricchio et al., represents a nonmagnetic scheme for δ-plutonium that, in contrast to DFT, relies upon one or more adjustable parameters. It remains to be seen if it can be applied also for the other phases, particularly the α-phase, of plutonium.

Further reading:

"Inhomogeneous Electron Gas," P. Hohenberg, W. Kohn, *Physical Review* 136 (1964).

"Self-Consistent Equations Including Exchange and Correlation Effects," W. Kohn, L.J. Sham, *Physical Review* 140 (1965).

"Calculated Ground State Properties of Light Actinide Metals and Their Compounds," M.S.S. Brooks, *Physica B* 130 (1985).

"Calculated Thermal Properties of Metals," V.L. Moruzzi et al., *Physical Review B* 37 (1988).

"Electronic Structure of α- and δ-Pu from Photoelectron Spectroscopy," A.J. Arko et al., *Physical Review B* 62 (2000).

"Density-Functional Investigation of Magnetism in δ-Pu," P. Söderlind et al., *Physical Review B* 66 (2002).

"Calculated Thermodynamic Properties of Plutonium Metal," G. Roberts et al., *Journal of Physics: Condensed Matter* 15 (2003).

"Monte Carlo Simulations of the Stability of delta-Pu," A. Landa et al., *Journal of Physics: Condensed Matter* 15 (2003).

"Density-Functional Calculations of α, β, γ, δ, δ′, and ϵ Plutonium," P. Söderlind, B. Sadigh, *Physical Review Letters* 92 (2004).

"Absence of Magnetic Moments in Plutonium," J.C. Lashley et al., *Physical Review B* 72 (2005).

"An Alternative Model for Electron Correlation in Pu," S.W. Yu et al., *Journal of Physics: Condensed Matter* 20 (2008).

"Exchange Energy Dominated by Large Orbital Spin-Currents in δ-Pu," F. Cricchio et al., *Physical Review B* 78 (2008).

"On the Electronic Configuration in Pu: Spectroscopy and Theory," J.G. Tobin et al., *Journal of Physics: Condensed Matter* 20 (2008).

"Quantifying the Importance of Orbital Over Spin Correlations in δ-Pu within Density-Functional Theory," P. Söderlind, *Physical Review B* 77 (2008).

UNCONVENTIONAL δ-PHASE STABILIZATION IN PLUTONIUM-GALLIUM ALLOYS

This article was contributed by Jeremy Mitchell, Franz Freibert, Daniel Schwartz, and Michael Bange, Materials Science and Technology Division, Los Alamos National Laboratory.

Face-centered cubic delta (δ)-phase plutonium stabilized with less than 3 atomic percent (at.%) gallium will partially transform martensitically to monoclinic alpha prime (α′) phase at cryogenic temperatures. Repeatedly alternating the temperature of young alloys in a dilatometer tends to stabilize δ plutonium by shifting the transformation to lower temperatures and reducing the amount of transformation. Similar experiments using samples aged naturally or by doping with plutonium-238 will stabilize δ plutonium such that annealing at or above 150 °C is required before normal transformation behavior occurs. We discuss the role that radiation damage and recovery play in this unconventional stabilization of δ-phase plutonium.

The first plutonium metallurgical studies during the Manhattan Project revealed that monoclinic α-phase plutonium is hard and brittle and therefore difficult to machine. The addition of as little as 1 at.% gallium, aluminum, cerium, americium, scandium, or indium was found to stabilize the softer, higher-temperature, face-centered cubic δ phase down to room temperature, thereby improving its manufacturing properties. Interestingly, this stabilization happens with the addition of elements with smaller (e.g., gallium) and larger (e.g., cerium) atomic radii than plutonium's.

Stabilization is thought to be due to the modification of plutonium's lattice spacing by these δ stabilizers, thus causing the 5f electrons to become more localized. At cryogenic temperatures and by applying pressure, gallium-stabilized δ-phase alloys can partially transform to the monoclinic α′ phase. We refer to the thermal variety as α'_t and the pressure-induced variety as α'_p. The general term α′ is used to distinguish pure α plutonium from this gallium-saturated allotrope that has a relatively expanded lattice.

The $\delta \rightarrow \alpha'_t$ transformation is martensitic, has a >150 °C hysteresis loop, and rarely exceeds 25% completion. The volume difference between pure δ and α plutonium is about 20%, so a complete $\delta \rightarrow \alpha'_t$ transformation is assumed to result in 20% volume contraction. The reverse transformation has proven to be a particularly rich area of investigation recently with the observation that it occurs in bursts.

During our investigations of the $\delta \rightarrow \alpha'_t$ transformation, we have found conditions of enhanced stabilization of the low-temperature δ-phase field. The two conditions we will discuss here are caused by (1) repeatedly alternating the temperature through the $\delta \leftrightarrow \alpha'_t$ forward and reverse transformations and (2) aging.

Three types of plutonium-2 at.% gallium materials were used in this study: an alloy that was several months up to 2 years; a naturally aged alloy that was 22 years old at the time of the experiments; and a plutonium-238-spiked alloy with

an accelerated equivalent age of 90 years. Dilatometry experiments included two types of temperature profiles: (1) repeatedly alternating from room temperature to between -150 and -165 °C and back up to 200–375 °C and (2) heating of the sample from room temperature to 120–200 °C before cooling to between -150 and -165 °C. The former profile was used to investigate the effects of repeated temperature alternation on the $\delta \rightarrow \alpha'_t$ transformation, whereas the latter was used to study possible aging effects on the transformation.

Transformation and reversion characteristics of young material.

experiment	cycle	maximum T before M_s (°C)	M_s (°C) [1]	α' (vol. %)	R_s (°C)	$\alpha' + \delta$ field (°C)[2]	R_f (°C)	$\alpha' \rightarrow \delta$ T range (°C)
04Pu0601[3]	1	RT	-133.6	17.8	48.5	203.5	80.4	31.9
	2	200	-164 (37.6 min.)	2.3	25.2	180.2	71.6	46.4
	3	200	-163.2 (33.1min.)	5.7	23.0	178.0	74.9	51.9
07Pu0901	1	RT	-129.8	12.5	47.6	202.6	80.8	33.2
	2	200	-167.3	9.1	38.2	193.2	72.9	34.7
	3	200	-167.4 (5.6 min.)	9.3	37.3	192.3	70.6	33.3
03Pu1401	1	RT	-124.7	13.5	39.9	194.9	90.5	50.6
	2	200	-155 (14.5 min.)	8.3	27.2	182.2	82.5	55.3
		2 hour RT rest						
	3	200	-155 (13.2 min.)	8.3	28.1	183.1	82.2	54.1
03Pu1402[4]	1	200	-155 (12.3 min.)	9.3	28.0	183.0	83.9	55.9
	2	200	-155 (35.7 min.)	2.7	6.1	161.1	80.1	74
	3	375	-142.5	8.3	19.3	174.3	80.3	61
03Pu1501	1	RT	-124.7	12.7	33.4	188.4	90.3	56.9
	2	300	-155.8 (3.7 min.)	6.8	23.8	178.8	79.8	56
		2 hour RT rest						
	3	300	-155 (0.6 min.)	9.5	28.3	183.3	83.3	55

1 = time required to transform during isothermal segment shown in parentheses
2 = defined here as the temperature range between the warmest isothermal in the data set (-155 °C) and the R_s
3 = heating rates through the transformation were 2.5, 5, and 7.5 °C/min for cycles 1, 2, and 3, respectively
4 = same sample as 03Pu1401 but run 18 hours after prior experiment
M_s = martensitic start temperature
R_s = reversion start temperature
R_f = reversion finish temperature
RT = room temperature

Results on young material

During a typical alternating-temperature dilatometer experiment on young material, the first martensitic transformation occurs at a higher temperature than the subsequent transformations, and the amount of transformation decreases or saturates as a function of repeated temperature alternation.

A plot of this behavior shows the hysteresis loop for a sample that has had its temperature cycled three times. In addition to a lower martensite start temperature (M_s) and less α'_t ingrowth, the second and third cycles have fewer prominent steps, or bursts in the dL/dt curve, during the reversion that are so obvious in the first cycle. The origin of bursting during the reversion is attributed to repeated autocatalysis followed by self-quenching.

The results of four separate experiments are compiled in the table on the facing page.

These experiments include the following temperature profiles: (1) alternating the temperature three times between cryogenic and 200 °C; (2) profile 1 with a two-hour room-temperature rest between cycles 2 and 3; (3) profile 1 with a 375 °C anneal between cycles 2 and 3; and (4) profile 1 with 300 °C anneals and a two hour room-temperature isothermal between cycles 2 and 3.

All of these experiments use the same plutonium-gallium alloy starting material from which the samples were extracted, although 07Pu0901 had been homogenized for 200 hours versus 50 hours for the other samples. Also note that experiment 03Pu1402 is the same sample as that used for 03Pu1401, and that the 03Pu1402 occurred 18 hours after 03Pu1401.

Observations from these experiments include the following:

- For samples that have not gone through repeated temperature alternation previously, the M_s for cycle 1 is higher than subsequent cycles.
- For samples that have not gone through repeated temperature alternation previously, the amount of α'_t is less in cycle 2 than cycle 1 and less than or equal to the cycle 2 amount during cycle 3.
- Room-temperature resting between cycles might allow for the reduction in α'_t ingrowth to saturate, but it does not restore normal transformation behavior after heating to 200 °C even after 18 hours.
- Annealing at or above 300 °C following cycle 1 allows the amount of α'_t transformation to increase, but not to the amount seen in cycle 1.
- Repeated temperature alternation shifts reversion start temperature (R_s) down by 10–20 °C and reversion finish temperature (R_f) down by 5–10 °C. This results in a contraction of the $\delta + \alpha'_t$ metastability field for these experimental conditions. Heating at or above 300 °C allows R_s and R_f to drift back up toward cycle 1 values.
- The increased homogenization of 07Pu0901 resulted in a higher R_s, lower R_f, and a smaller temperature range during which the reverse transformation takes place.

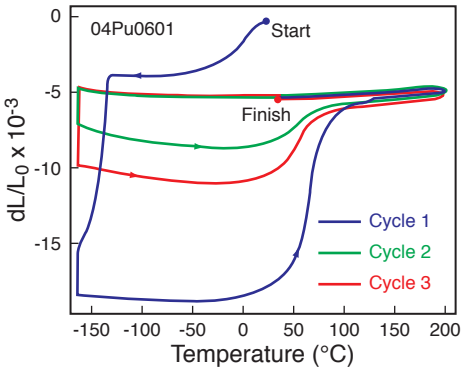

Above: Dilatometry of a 1-year-old sample during three cycles between -165 and 200 °C. Note the decrease in % α′ and lower M_s as a function of repeated temperature alternation. The contraction during the first cooling segment before transformation was caused by a temporary cooling irregularity. Below: Detail of the dL/dt curve through the reverse transformation of the experiment. Dilation behavior uses the scale on the left, burst behavior uses the scale on the right.

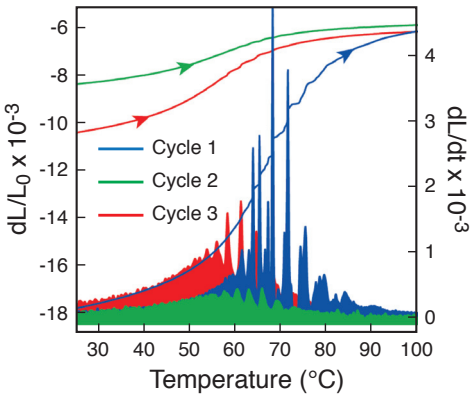

Transformation and reversion characteristics of naturally and accelerated-aged (AAP02KL29) material.

Results on old material

The following table summarizes a series of experiments performed on naturally—and accelerated—aged plutonium samples.

experiment	cycle	maximum T before M_s (°C)	M_s (°C)[1]	α′ (vol. %)	R_s (°C)	α′+ δ field (°C)	R_f (°C)	α → δ T range (°C)
06Pu0301	1	RT	-	-	-	-	-	-
	2	200	-150.1	7.4	4.8	159.8	133.5	128.7
	3	200	-147.4	4.6	-3	152	130.1	133.1
AAP02KL29	1	45[1]	-	-	-	-	-	-
	2	375	-127.9	5.3	30.9	185.9	96.5	65.6
	3	375	-133.3	0.40	-	-	-	-
06Pu0402[2]	-	120	-	0.84	-17.7	137.3	105.5	123.2
06Pu0501[2]	-	140	-	1.4	5.4	160.4	-	-
06Pu0601	-	160	-146.8	6.9	8.2	163.2	108.3	100.1
06Pu0701	-	180	-144.6	7.2	4.8	159.8	138.8	134
06Pu0201	-	200	-140.1	8.2	32	187	96.6	64.6

1 = storage temperature for plutonium-238-spiked alloys
2 = transformation is minimal and difficult to quantify
M_s = martensitic start temperature
R_s = reversion start temperature
R_f = reversion finish temperature
RT = room temperature

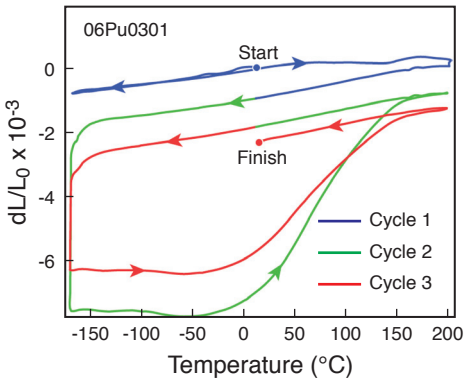

Dilatometry of a 22-year-old sample during cycling between -165 and 200 °C. Note the lack of transformation in cycle 1 compared to subsequent cycles.

We were surprised to find that during the cycling experiments both types of aged material do not transform during cooling to below -155 °C. Only after heating up to 200 °C or greater and cooling down during cycle 2 is the transformation observed. Normal repeated temperature alternation-assisted stabilization follows the second cycle, although the M_s is slightly higher on the third cool down for naturally aged material and slightly lower for the accelerated-aged material

As with the experiments summarized in the first table, repeatedly alternating the temperature lowers R_s and R_f and contracts the $\delta + \alpha'_t$ metastability field. When compared to the young material, the aged samples show much less α′ ingrowth, lower R_s and R_f, a much larger reverse transformation temperature range, and a smaller $\delta + \alpha'_t$ metastability field. In general, the aged samples are more δ-phase stable than the newer alloys.

To better understand the lack of transformation during the first cycle in naturally aged materials, we performed a series of experiments to identify the

minimum annealing temperature that unlocks normal transformation behavior. These experiments began with a heating phase of 120–200 °C, followed by cooling to -165 °C to observe the $\delta \rightarrow \alpha'_t$ transformation.

Experiments that started with an anneal at 120 or 140 °C showed very slight indication of the transformation. Analysis of the dL/dt during the reverse transformation temperature range and comparing these results to the cycled samples suggests that 0.8 and 1.4 vol. %, respectively, transformed in these two experiments. The samples heated above 140 °C showed much more transformation, an increase from 6.9 to 8.2% during the temperature range 160–200 °C. The largest increase is seen between the 140 and 160 °C annealing experiments.

Discussion

In addition to more conventional solute stabilization of δ-phase, repeated temperature alternation and aging can act to enhance δ over a limited temperature range. In the case of repeated temperature alternation, $\delta \leftrightarrow \alpha'_t$ causes plastic deformation in δ and results in a high dislocation density. Transmission electron microscopy of similarly cycled material has shown that the dislocation density of samples heated at 300 °C for 4 hours is reduced 86 times in the highly damaged regions near the α'_t plates.

Previous experiments on samples transformed using isostatic pressure showed that annealing at 440 °C for 200 hours was needed before the thermally induced transformation would occur, suggesting that significant gallium diffusion is required to fully reset the microstructure to the pretransformation condition.

Our results on aged alloys suggest that gallium-stabilized δ-phase is further stabilized by the presence of lattice defects accumulated over many years of self-irradiation. These defects anneal out somewhere between room temperature and 200 °C, with our differential scanning calorimetry (DSC) and dilatometry work suggesting a narrower range of 140–150 °C. Specimens heated to 200 °C, and therefore free of these defects, undergo significant transformation to α'_t when cooled.

Subsequent cycles with a maximum temperature of 200°C result in less transformation to α'_t, due to the formation of new δ-stabilizing defects by the transformation-reversion process. Heating the material to 375 °C removes most of these defects, and specimens heated to this temperature again show large amounts of α′ formation when cooled.

Based on their DSC experiments, Blobaum et al., in an article published in *Acta Materialia* in 2006, proposed that room-temperature conditioning allows for incipient eutectoid decomposition of gallium-stabilized δ-phase plutonium to $\alpha + Pu_3Ga$. This effect saturates after six hours and the resulting α embryos provide nuclei for α'_t during subsequent cooling.

However, we believe that there is no dilatometry evidence from the data presented here that room-temperature conditioning between cycles allows for the return of normal and reproducible transformation behavior, even after as

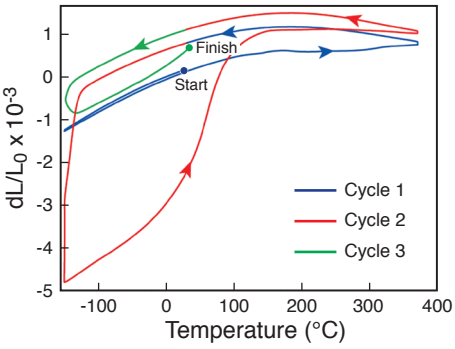

Dilatometry of a plutonium-238-spiked plutonium-gallium alloy (sample AAP02KL29) during repeated cycling between -150 and 200 °C. Note the lack of transformation in cycle 1 compared to subsequent cycles and the large decrease in α′ between cycles 2 and 3.

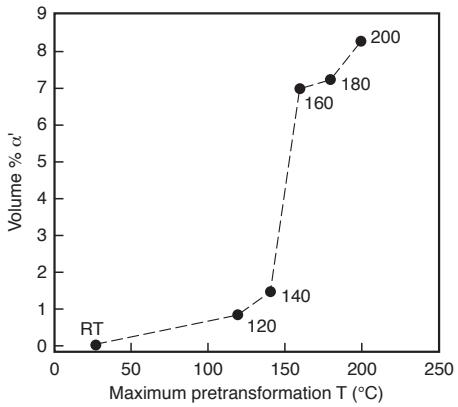

Compilation of α′ ingrowth measurements in 22-year-old samples. Samples were annealed at progressively higher temperatures (x-axis) and cooled to -165 °C to allow for the transformation to occur.

This work was funded by the DOE under contract W-7405-ENG-36.

much as 18 hours of resting between cycles. In fact, what we consider to be normal transformation behavior does not return until a sample has been heated close to 400 °C.

It is important to consider that the temperature profiles of our measurements do not exactly match those for the prior DSC experiments, so direct comparison between this study and that of Blobaum et al. is limited. However, the discrepancy between these results may reflect differences in samples or the measurement technique (i.e., heat release vs. length change). Additionally, samples in this study, unless indicated otherwise, were used once, whereas those in the DSC experiments were used in dozens of separate measurements.

Further reading:

"Evidence of Transformation Bursts During Thermal Cycling of a Pu-Ga Alloy," K.J.M Blobaum et al., *Metallurgical and Materials Transactions* 37A (2006).

"Nucleation and Growth of the α′ Martensitic Phase in Pu–Ga Alloys," K.J.M. Blobaum et al., *Acta Materialia* 54 (2006).

"Orientation Relationship, Habit Plane, Twin Relationship, Interfacial Structure, and Plastic Deformation Resulting from the $\delta \rightarrow \alpha'$ Isothermal Martensitic Transformation in Pu-Ga Alloys," K.T. Moore et al., *Metallurgical and Materials Transactions* 38A (2007).

"Phase Stability and Phase Transformations in Pu–Ga Alloys," S.S. Hecker et al., *Progress in Materials Science* 49 (2004).

"Phase Stability and Phase Transformations in Plutonium and Plutonium-Gallium Alloys," J.N. Mitchell et al., *Metallurgical and Materials Transactions* 35A (2004).

EXPANDING THE PLUTONIUM LATTICE IN A QUEST FOR MAGNETISM

This article was contributed by Michael Fluss and Scott McCall, Condensed Matter and Materials Division, Lawrence Livermore National Laboratory, and Chris Marianetti, Department of Applied Physics and Applied Mathematics, Columbia University.

The lanthanides, elements with partially filled 4f electron orbitals, display a rich variety of magnetic ordering and are generally well understood as examples of local moment systems because the 4f orbitals are pulled in tightly around the nucleus, thus having little overlap with neighboring atoms and not bonding.

The ordered magnetism can be suppressed by applying pressure, which increases the overlap of the metallic bonding electrons, thereby broadening the conduction band so that 4f electrons no longer couple effectively through the RKKY interaction yet still remain localized. (RKKY stands for Ruderman-Kittel-Kasuya-Yosida and in a metal refers to the interaction of magnetic spins mediated by conduction electrons.)

A very elegant example of this is the recent high-pressure work on gadolinium by D.D. Jackson et al., which at ambient pressure orders ferromagnetically at room temperature, but when compressed to ~89% of its initial volume, loses all indication of long-range magnetic order.

Additional pressure, about 60 giga pascals (GPa) for gadolinium, squeezes the volume to half its initial value and results in significant overlapping of the 4f electron orbitals, which thus become bandlike, removing local moments completely. By increasing the degree of 4f orbital overlap in the lanthanides, they can be driven from ordered magnets to local moment paramagnets, which display Curie behavior as a function of temperature: $\chi(T) = C/T$, and then finally to itinerant paramagnets, where the electrons delocalize and the magnetic susceptibility becomes much smaller and temperature independent: $\chi(T) = \chi_o$.

The actinides are the 5f analogs of the lanthanides, and similar localized behavior is observed in the heavy actinides—americium (Am) and beyond, where, as in the lanthanides, the 5f orbitals have little overlap with their neighbors. However, the circumstances are quite different for the lighter actinides where smaller atomic volumes create significant overlap among 5f orbitals on neighboring atoms, which thereby participate in metallic bonding. This overlap leads to itinerancy in the 5f electrons, naturally eliminating local moments, and is consistent with the absence of magnetism in any of the light-actinide metals.

The crossover between the itinerant light actinides and localized behavior of the heavy actinides occurs between plutonium, with an atomic volume of 20.2 cubic angstroms ($Å^3$) at room temperature and the much larger 29.3 $Å^3$ atomic volume of americium.

Because the localized 5f electrons of americium fill the $J_{5/2}$ sublevel, the local moments cancel completely, thus J = 0 and there is no long-range order. Instead, the primary contribution to the magnetic susceptibility is a large temperature-independent contribution known as the Van Vleck contribution, which arises from an excited state close in energy to the ground state. This is a single-ion effect, and thus is insensitive to the local environs of the americium atom.

Editor's note: The effects of pressure on the delocalization of 5f electrons in americium have been an ongoing dialogue of the Plutonium Futures conference. For more information on the crystal structures of americium phases and the influence of pressure on atomic volumes, see articles by Richard Haire (ARQ 3rd/4th Quarters 2003) and Jean-Claude Griveau (ARQ 3rd/4th Quarters 2006).

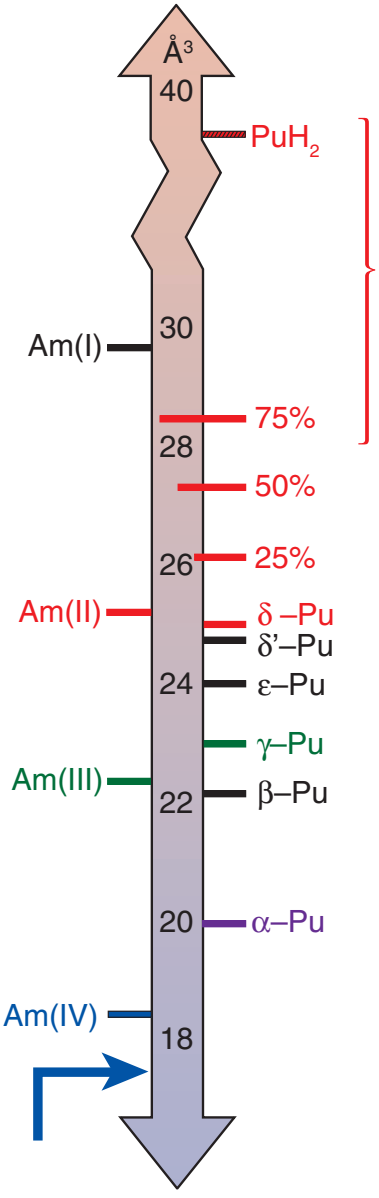

Volume phase diagram for americium under pressure on the left side and plutonium as a function of temperature and doping on the right side. The blue arrow shows where the 5f electrons of americium delocalize, while the red bracket indicates the range in which the 5f plutonium electrons may localize. The percentages refer to the $Pu_{1-x}Am_x$ alloys.

With increasing pressure, americium passes into lower symmetry crystal structures with Am(III) becoming orthorhombic like gamma (γ)-plutonium, while Am(IV) has the even more distorted Pnma structure of alpha (α)-uranium (U). Yet like its 4f analog gadolinium, the 5f electrons do not delocalize until the volume is significantly reduced—to about 60% of its zero pressure volume for americium—as indicated by the precipitous loss of superconductivity well after transformation to the Am(IV) phase.

While americium differs from plutonium in the number of 5f electrons, they are adjacent to one another in the periodic table. This naturally leads to a question: if reducing the volume of americium leads to delocalization, is it possible to increase the volume of plutonium and thereby localize the 5f elections, perhaps eventually leading to magnetic ordering?

This is not a new idea, and indeed it was suggested that this might be exactly what happens at delta (δ)-plutonium, which has a volume 20% larger than the room-temperature α-phase, and can be stabilized to low temperatures with the addition of a few atomic percent gallium or aluminum. However, a number of measurements contradict the assertion of localization, most convincingly the magnetic susceptibility that increases by about 10% but remains largely temperature independent—an indication that the 5f electrons are still itinerant and contribute to the Pauli susceptibility while the increase implies that the conduction bands have begun to narrow.

Thus, the expansion from 20.2 $Å^3$ for α-plutonium to 24.8 $Å^3$ for δ-plutonium does not localize the 5f electrons, but the narrowing of the conduction bands is a precursor, suggesting that they might become localized if further expanded. Indeed, in the case of plutonium hydride (PuH_2), which if the hydrogen ions are ignored, has the same face-centered cubic structure as δ-plutonium but with a much expanded volume of ~38.6 $Å^3$, the 5f electrons of plutonium are not only localized but order antiferromagnetically at 30K. Furthermore, simple density-functional theory (DFT) calculations show a minimal change in the f-electron count, justifying neglect of the hydrogen in considering the magnetic properties.

A second, more systematic approach to expanding the plutonium lattice is by applying negative pressure through alloying with americium, where the δ-plutonium structure is stable from 6 to 80% americium and expands a further 20% beyond the volume of δ-plutonium at the upper limit of americium. Because the only contribution of the americium atoms to the magnetic susceptibility should be a Van Vleck contribution independent of the local environment, it can be easily removed from the susceptibility of each alloy. Of course, alloying does not simply expand the plutonium atomic volume but should also reduce the number of 5f electrons in the conduction band because the americium 5f electrons remain localized in a closed sublevel.

When samples in the vicinity of 25% americium are measured, a significant increase in the magnetic susceptibility is observed, indicating that the 5f bands continue to narrow but do not yet show signs of localization. These results are

very consistent with our theoretical work using dynamical mean field theory (DMFT), where for the first time the values of the magnetic susceptibility as a function of temperature and volume have been calculated.

This study finds that for the δ-plutonium structure with its normal volume of 24.8 Å^3, the magnetic susceptibility is flat, indicative of Pauli paramagnetism. By expanding the lattice to 28.8 Å^3, the magnetic susceptibility increases more than 50%, indicative of narrowing bands and consistent with observations of the plutonium-americium alloys. Using DMFT to further expand the lattice to 32.8 Å^3 results in a Curie-like (χ=C/T) susceptibility reflecting localization of the 5f electrons similar to what is observed experimentally at the volume of PuH_2.

A DMFT study that alloys americium into plutonium has been performed by J.H. Shim et al. They show that the degree of localization is a competition between the americium-induced volume expansion and decreasing the number of 5f electrons, n_f, due to americium doping, both of which enhance localization, and the chemical presence of americium, which enhances itinerancy. They predict the net effect is that the itinerancy slightly increases (i.e., localization decreases) as americium is doped into plutonium.

However, our experiments at 25% americium indicate the opposite. Given that DMFT predicts a delicate balance of effects, further DMFT studies should be performed to explore the sensitivity of these results. Furthermore, exact continuous time quantum Monte Carlo (QMC) calculations would be indispensable, as demonstrated in our previous work, where the susceptibility can be directly calculated.

Ultimately, it will be critical to perform the experiment at 75% americium, given that the 25%-americium sample shows enhanced magnetic susceptibility. While a significant challenge, understanding this will serve as an excellent benchmark for theoretical models such as DMFT.

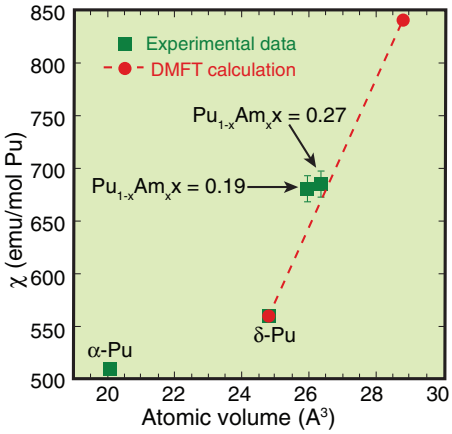

The temperature-independent magnetic susceptibility measured as a function of atomic volume. The red data are values calculated from DMFT scaled to the measured value of δ-plutonium. The line is a guide to the eye.

Further reading:

"Electronic Coherence in δ-Pu: A Dynamical Mean-Field Theory Study," C.A. Marianetti et al., *Physical Review Letters* 101 (2008).

"High-Pressure Magnetic Susceptibility Experiments on the Heavy Lanthanides Gd, Tb, Dy, Ho, Er, and Tm," D.D. Jackson et al., *Physical Review* B 71 (2005).

"Screening of Magnetic Moments in PuAm Alloy: Local Density Approximation and Dynamical Mean Field Theory Study," J.H. Shim et al., *Physical Review Letters* 101 (2008).

"Superconductivity in the Americium Metal as a Function of Pressure: Probing the Mott Transition," J.C. Griveau et al., *Physical Review Letters* 94 (2005).

"Theoretical and Experimental Studies on Gadolinium at Ultra High Pressure," H. Hua et al., *The Review of High Pressure Science and Technology* 73 (1998).

This work was performed by Lawrence Livermore National Laboratory under the auspices of the DOE under contract DE-AC52-07NA27344.


Finis

Actinide Research Quarterly
is published by Los Alamos
National Laboratory

Actinide Research Quarterly

is a publication of the
Stockpile Manufacturing and
Support (SMS) Directorate.
The directors of the Seaborg Institute for
Transactinium Science serve as the magazine's
scientific advisors. *ARQ* highlights progress
in actinide science in such areas as process
chemistry, metallurgy, surface and separation
sciences, atomic and molecular sciences,
actinide ceramics and nuclear fuels,
characterization, spectroscopy, analysis,
and manufacturing technologies.

Address correspondence to
Actinide Research Quarterly
c/o Meredith Coonley
Mail Stop G756
Los Alamos National Laboratory
Los Alamos, NM 87545

ARQ can be read online at www.lanl.gov/arq

If you have questions, comments, suggestions,
or contributions, please contact the
ARQ staff at arq@lanl.gov.

Phone (505) 667-0392
Fax (505) 665-7895

Errata

ARQ regrets the following errors that appeared in the previous issue:

In a discussion of nitric acid processing on page 6, we incorrectly stated that PuO_2 produced from Pu(III) oxalate can be used directly for production of mixed-oxide (MOX) nuclear fuels. For the currently established process for production of MOX fuels, Pu(IV) oxalate is precipitated and calcined to PuO_2.

In the discussion of americium-241 ingrowth on page 12, we said the half-life of plutonium-241 is 13.2 years; the half-life is 14.35 years.

LALP-09-013


Los Alamos
NATIONAL LABORATORY
EST.1943